Chem Soc Rev

REVIEW ARTICLE

View Article Online
View Journal | View Issue

Open Access Article. Published on 24 June 2014. Downloaded on 1/3/2025 11:41:55 PM.
This article is licensed under a Creative Commons Attribution 3.0 Unported Licence.

Cite this: *Chem. Soc. Rev.*, 2014, **43**, 7887

Received 27th May 2014

DOI: 10.1039/c4cs00189c

www.rsc.org/csr

Heterogeneous catalysis for sustainable biodiesel production *via* esterification and transesterification

Adam F. Lee,* James A. Bennett, Jinesh C. Manayil and Karen Wilson

Concern over the economics of accessing fossil fuel reserves, and widespread acceptance of the anthropogenic origin of rising CO_2 emissions and associated climate change from combusting such carbon sources, is driving academic and commercial research into new routes to sustainable fuels to meet the demands of a rapidly rising global population. Here we discuss catalytic esterification and transesterification solutions to the clean synthesis of biodiesel, the most readily implemented and low cost, alternative source of transportation fuels to meet future societal demands.

1. Introduction

Sustainability, in essence the development of methodologies to meet the needs of the present without compromising those of future generations, has become a watchword for modern society, with developed and developing nations and multinational corporations promoting international research programmes into sustainable food, energy, materials, and even city planning. In the context of energy, despite significant growth in proven and predicted fossil fuel reserves over the next two decades, notably heavy crude oil, tar sands, deepwater wells, and shale oil and gas, there are great uncertainties in the economics of their exploitation *via* current extraction methodologies, and crucially, an increasing proportion of such carbon resources (estimates vary between 65–80%[1–3]) cannot be burned without breaching the UNFCC targets for a 2 °C increase in mean global temperature relative to the pre-industrial level.[4,5] There is clearly a tightrope to walk between meeting rising energy demands, predicted to climb 50% globally by 2040[6] and the requirement to mitigate current CO_2 emissions and hence climate change. Similar considerations

European Bioenergy Research Institute, Aston University, Aston Triangle, Birmingham B4 7ET, UK. E-mail: a.f.lee@aston.ac.uk; Tel: +44 (0)121 2044036

Adam F. Lee

Adam Lee is Professor of Sustainable Chemistry and an EPSRC Leadership Fellow in the European Bioenergy Research Institute, Aston University. He holds a BA (Natural Sciences) and PhD from the University of Cambridge, and following post-doctoral research at Cambridge and Lecturer/Senior Lecturer roles at the Universities of Hull and York respectively, held Chair appointments at Cardiff, Warwick and Monash universities. His research addresses the rational design of nanoengineered materials for clean catalytic technologies, with particular focus on sustainable chemical processes and energy production, and the development of in situ methods to provide molecular insight into surface reactions, for which he was awarded the 2012 Beilby Medal and Prize by the Royal Society of Chemistry.

James Bennett

Dr James Andrew Bennett obtained his Master and PhD at the University of Leicester, where he investigated the use of perfluoroalkyl moieties to allow heterogenisation of homogeneous catalysts over zirconium phosphonate supports. He then worked at the University of Birmingham, researching biogenic heterogeneous catalysts composed of transition metal nanoparticles supported on bacterial biomass, using waste sources of metals and biomass to produce "green" catalyst materials. He is currently working with Professors Karen Wilson and Adam Lee at the European Bioenergy Research Institute at Aston University, developing environmentally sustainable catalysts derived from industrial waste for pyrolysis oil upgrading.

Open Access Article. Published on 24 June 2014. Downloaded on 1/3/2025 11:41:55 PM.
This article is licensed under a Creative Commons Attribution 3.0 Unported Licence.

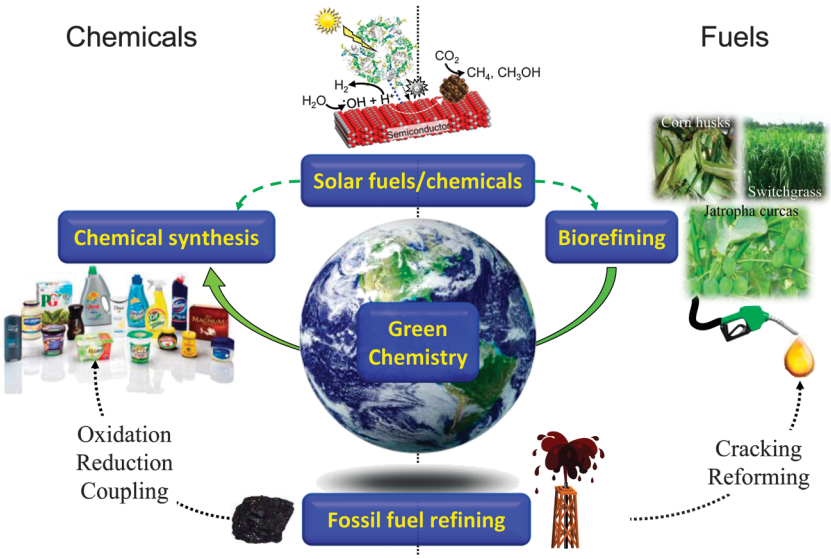

Scheme 1 Current and future roles for heterogeneous catalysis in the production of sustainable chemicals and fuels.

apply to ensuring a continued supply of organic materials for applications including polymers, plastics, pharmaceuticals, optoelectronics and pesticides, which underpin modern society, and for which significant future growth is anticipated, tracking the predicted four-fold rise in global GDP and associated requirements for advanced consumer products by 2050.[7] The quest for sustainable resources to meet the demands of a rapidly rising world population represents one of this century's grand challenges.[8,9] Heterogeneous catalysis has a rich history of facilitating energy efficient selective molecular transformations and contributes to 90% of chemical manufacturing processes and to more than 20% of all industrial products.[10,11] In a post-petroleum era, catalysis will be central to overcoming the engineering and scientific barriers to economically feasible routes to alternative source of both energy and chemicals, notably bio-derived and solar-mediated *via* artificial photosynthesis (Scheme 1).

While many alternative sources of renewable energy have the potential to meet future demands for stationary power generation, biomass offers the most readily implemented, low cost solution to a drop-in transportation fuel for blending with/replacing conventional diesel[12] *via* the biorefinery concept, illustrated for carbohydrate pyrolysis/hydrodeoxygenation (HDO)[13,14] or lipid transesterification[15,16] to alkanes and biodiesel respectively in Scheme 2. First-generation bio-fuels derived from edible plant materials received much criticism over the attendant competition between land usage for fuel crops *versus* traditional agricultural cultivation.[17] Deforestation practices, notably in Indonesia, wherein vast tracts of rainforest

Jinesh C. Manayil

Dr Jinesh Manayil obtained his MSc in Chemistry from Mahatma Gandhi University in 2004, prior to a MTech in Industrial Catalysis from Cochin University of Science and Technology in 2007. He subsequently undertook postgraduate research in catalytic and ion-exchange applications of layered double hydroxides, receiving his PhD in 2012 from the Central Salt and Marine Chemicals Research Institute (CSIR-CSMCRI), India under the supervision of Dr Kannan Srinivasan. He is currently a Research Associate with Professors Karen Wilson and Adam Lee at the European Bioenergy Research Institute at Aston University, where he is developing solid acid-base catalysts for biomass mass conversion.

Karen Wilson

Karen Wilson is Professor of Catalysis and Research Director of the European Bioenergy Research Institute at Aston University, where she holds a Royal Society Industry Fellowship. Her research interests lie in the design of heterogeneous catalysts for clean chemical synthesis, particularly the design of tunable porous materials for sustainable biofuels and chemicals production from renewable resources. She was educated at the Universities of Cambridge and Liverpool, and following postdoctoral research at Cambridge and the University of York, was appointed a Lecturer and subsequently Senior Lecturer at York, prior to appointment as a Reader in Physical Chemistry at Cardiff University.

 This journal is © The Royal Society of Chemistry 2014

Open Access Article. Published on 24 June 2014. Downloaded on 1/3/2025 11:41:55 PM.
This article is licensed under a Creative Commons Attribution 3.0 Unported Licence.

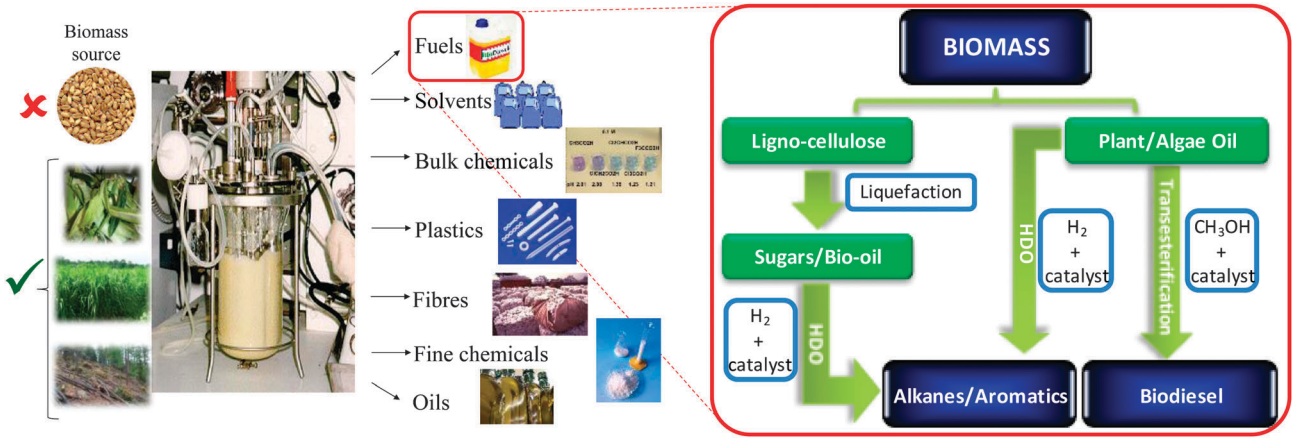

Scheme 2 Biorefinery routes for the co-production of chemicals and transportation fuels from biomass.

and peat land have been cleared to support palm oil plantations, have also provoked controversy.[18] To be considered sustainable, second generation bio-based fuels and chemicals are sought that use biomass sourced from non-edible components of crops, such as stems, leaves and husks or cellulose from agricultural or forestry waste. Alternative non-food crops such as switchgrass or *Jatropha curcas*,[19] which require minimal cultivation and do not compete with traditional arable land or drive deforestation, are other potential candidate biofuel feedstocks. There is also growing interest in extracting bio-oils from aquatic biomass, which can yield 80–180 times the annual volume of oil per hectare than that obtained from plants.[20] Around 9% of transportation energy needs are predicted to be met *via* liquid biofuels by 2030.[21]

Biodiesel is a clean burning and biodegradable fuel which, when derived from non-food plant or algal oils or animal fats, is viewed as a viable alternative (or additive) to current petroleum-derived diesel.[22] Commercial biodiesel is currently synthesised *via* liquid base catalysed transesterification of C_{14}–C_{20} triacylglyceride (TAG) components of lipids with C_1–C_2 alcohols[23–26] into fatty acid methyl esters (FAMEs) which constitute biodiesel as shown in Scheme 3, alongside glycerol as a potentially valuable by-product.[27] While the use of higher (*e.g.* C_4) alcohols is also possible,[28] and advantageous in respect of producing a less polar and corrosive FAME[29] with reduced cloud and pour points,[30] the current high cost of longer chain alcohols, and difficulties associated with separating the heavier FAME product from unreacted alcohol and glycerol, remain problematic. Unfortunately, homogeneous acid and base catalysts can corrode reactors and engine manifolds, and their removal from the resulting biofuel is particularly problematic and energy intensive, requiring aqueous quench and neutralisation steps which result in the formation of stable emulsions and soaps.[12,31,32] Such homogeneous approaches also yield the glycerine by-product, of significant potential value to the pharmaceutical and cosmetic industries, in a dilute aqueous phase contaminated by inorganic salts. The utility of solid base and acid catalysts for biodiesel production has been widely reported,[15,25,33–41] wherein they offer

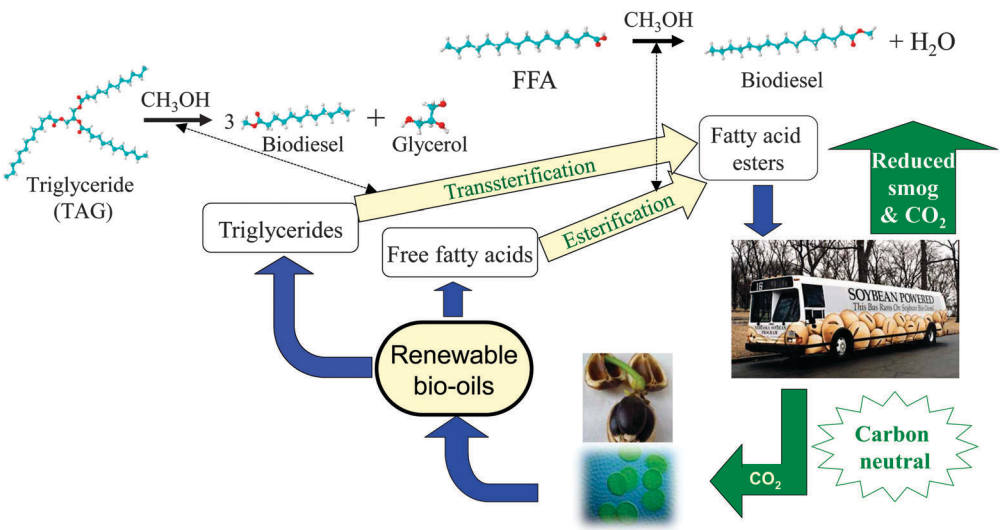

Scheme 3 Biodiesel production cycle from renewable bio-oils *via* catalytic transesterification and esterification.

Open Access Article. Published on 24 June 2014. Downloaded on 1/3/2025 11:41:55 PM.
This article is licensed under a Creative Commons Attribution 3.0 Unported Licence.

improved process efficiency by eliminating the need for quenching steps, allowing continuous operation,[42] and enhancing the purity of the glycerol by-product. Technical advances in catalyst and reactor design remain essential to utilise non-food based feedstocks, and thereby ensure that biodiesel remains a key player in the renewable energy sector for the 21st century. In this review, we highlight the contributions of tailored solid acid and base catalysts to catalytic biodiesel synthesis *via* TAG transesterification to FAMEs and free fatty acid (FFA) esterification.

2. Feedstocks for biodiesel

The feedstock sources employed for biodiesel synthesis have remained little changed since the first engine tests with vegetable oils in the late 1800s,[43] and are normally classified as either first or second generation,[44,45] the latter oft referred to as a source of 'advanced biofuels'. First generation biodiesel is derived from edible vegetable oils such as soya, palm,[46] oil seed rape[47] and sunflower,[48] however the attendant poor yields (typically 3000–5000 L hectare^{-1} year^{-1}) and socio-political concern over the diversion of such food crops for fuels has led to their fall from favour within Europe and North America. Second generation biodiesel is normally considered to be that obtained from non-edible oils such as castor,[49] Jatropha[50] and neem,[51] microalgae,[44,52] animal fats (*e.g.* tallow and yellow grease),[53] or waste oils including organic components of municipal waste:[54] these offer lower greenhouse gas emissions,[45] *e.g.* 150 g_{CO_2} MJ^{-1} for African biodiesel from Jatropha exported to the EU with attendant use of residual seedcake as a fertiliser *versus* 220 g_{CO_2} MJ^{-1} for Mexico biodiesel from Jatropha without attendant methane capture;[55] improved environmental and energy life cycles;[56] and superior biodiesel yields (upto 100 000 L hectare^{-1} year^{-1} for microalgae). Commercial biodiesel is require to meet a range of national and international standards, the most widely conformed to being the American standard ASTM D6751,[57] and the European standard EN 14214:[58] the high free fatty acid of some non-edible oils can lower the FAME content below accepted standards,[59] whereas feedstocks like *Brassica carinata* and *Jatropha curcas* have comparable or even higher oil content than many edible oils.[15]

Interest in biodiesel production soared following the global oil crisis of the 1970s, resulting in the United States, European Union, Brazil, China, India, and South Africa convening a UN International Biodiesel Forum for biodiesel development. Today, the United States, European Union and Brazil, alongside Malaysia, remain leading forces in the biodiesel market. Current industrial production is dominated by the utilisation of edible vegetable oils such as soybean (7.08 million), palm (6.34 million), rapeseed (6.01 million), castor, coconut and *Jatropha curcas* oil. The primary cost of biodiesel lies in the raw material, and since the market is dominated by food grade oils,[59] which are significantly more expensive than petroleum-derived diesel, economic viability remains to be proven. Use of the surplus from edible oil production may assist countries to meet the demands for biodiesel production without negatively impacting upon food requirements.[60] Feedstock selection is a strong function of local availability. Soybean oil, which is widely used in the United States and South America, is the third largest feedstock for biodiesel after rapeseed oil in Europe and palm oil in Asian countries, such as Malaysia and Indonesia, which also use sunflower and coconut oil, with *Jatropha curcas* oil widespread across South East Asia.[61] Soybean and rapeseed oils account for about 85% of global biodiesel production,[62] with 75% of total biodiesel produced in Europe. Competition for land to produce biodiesel feedstocks is problematic, hence maximising the yield of oil from a given feedstock is critical. Edible soybean seed consists of 20% oil *versus* rapeseed at 40%, whereas non-edible Jatropha and Karanja seeds contain around 40% and 33% oil respectively.[60] Adoption of soybean (as in the US) as a global biodiesel feedstock would be problematic, not only due to competition for its use as a food crop, but also the high quantities of waste, associated with its low oil yield, although this could be mitigated by the introduction of the oil seed cake as a major animal feed. The oil yield from non-edible Jatropha is particularly noteworthy since it can grow in poor quality soil and waste land, avoiding competition with arable land for food crops, however harvesting of the toxic seeds is labour intensive.[63] Around 15 million tons of waste cooking/frying oils is disposed of annually worldwide. Such low cost feedstocks, could meet a significant portion of current biodiesel demands, however chemical changes occurring during cooking which increase their FFA and moisture content must be taken into consideration.[64] Recent studies suggest that the production cost of biodiesel could be halved through waste cooking oils in comparison with virgin oils.[65] However because of its high melting point and viscosity, and less predictable supply, waste cooking oil has been less extensively investigated than vegetable oils.[31] Algal biomass has received considerable recent attention, since lipids from algae can be used for biodiesel production *via* conventional transesterification technologies. Microalgae are fast-growing and produce higher oil yields than plant counterparts. The high oil content of different microalgae favours their commercialisation as a promising feedstock: one acre of microalgae can produce 5000 gallons of biodiesel annually compared to only 70 gallons from an equivalent area of soybean,[52] and algae can flourish on land unusable for plant cultivation and without fresh water. Algal oil yields vary with the species, nutrient supply and harvest time,[66] however the properties of the resulting FAMEs are not superior to those derived from plant oils, and further research into algal oils rich in saturated long chain fatty acids is required in order to improve the quality of the final biodiesel.[67]

The choice of oil feedstock in turn influences the biodiesel composition and hence fuel properties,[43,68] notably acid value, oxidation stability, cloud point, cetane number and cold filter plugging point. Oils from plants usually comprise five major fatty acids components: palmitic (16 : 0); stearic (18 : 0); oleic (18 : 1); linoleic (18 : 2); and linolenic (18 : 3). Table 1 illustrates their distribution and associated physicochemical properties for some common feedstocks. High FFA oils not only compromise base catalysed transesterification and hence biodiesel yields, but can corrode engines and ancillary machinery; the acceptable acid range is between 0.5–3%.[60] The cetane number (CN), a measure of diesel ignition quality, is higher for biodiesel (46–52) than that of conventional diesel (40–55), with the international

 This journal is © The Royal Society of Chemistry 2014

Open Access Article. Published on 24 June 2014. Downloaded on 1/3/2025 11:41:55 PM.
This article is licensed under a Creative Commons Attribution 3.0 Unported Licence.

Table 1 Common feedstocks for biodiesel production, free fatty acid composition and physicochemical properties. Reprinted from ref. 59, Copyright (2010), with permission from Elsevier

	Feedstock	Composition/wt% fatty acid	Density/ g cm^3	Flash point/°C	Acid value mg KOH g^{-1}	Heating value/MJ kg^{-1}
Edible oils	Soybean	C16:0, C18:1, C18:2	0.91	254	0.2	39.6
	Rapeseed	C16:0, C18:0, C18:1, C18:2	0.91	246	2.92	39.7
	Sunflower	C16:0, C18:0, C18:1, C18:2	0.92	274	—	39.6
	Palm	C16:0, C18:0, C18:1, C18:2	0.92	267	0.1	—
	Peanut	C16:0, C18:0, C18:1, C18:2, C20:0,C22:0	0.90	271	3	39.8
	Corn	C16:0, C18:0, C18:1, C18:2, C18:3	0.91	277	—	39.5
	Camelina	C16:0, C18:0, C18:1, C18:2, C18:3, C20:0, C20:1, C20:3	0.91	—	0.76	42.2
	Cotton	C16:0, C18:0, C18:1, C18:2, C18:3	0.91	234	—	39.5
Non-edible oils	*Jatropha curcas*	C16:0, C16:1, C18:0, C18:1, C18:2	0.92	225	28	38.5
	Pongamina pinnata	C16:0, C18:0, C18:1, C18:2, C18:3	0.91	205	5.06	34
	Palanga	C16:0, C18:0, C18:1, C18:2	0.90	221	44	39.25
	Tallow	C14:0, C16:0, C16:1, C17:0, C18:0, C18:1, C18:2	0.92	—	—	40.05
	Poultry	C16:0, C16:1, C18:0, C18:1, C18:2, C18:3	0.90	—	—	39.4
	Used cooking oil	Depends on fresh cooking oil	0.90	—	2.5	—

standard specified in ASTM D6751 and EN 14214 at 47 and 51 respectively. Cetane number varies with the degree of oil unsaturation and chain length. Esters of palmitic and stearic acid possess CNs higher than 80, while that of oleate is 55–58, with CN generally decreasing with increasing unsaturation (*e.g.* CN = 40 for linoleic and 25 for linolenic acid), falling to 48-5 for soybean- and 52–55 for rapeseed-derived biodiesel.[69] Fatty acid chain composition also influences NO_x emissions, with biodiesel containing esters of saturated fatty acids emitting less NO_x than petroleum diesel, and emissions increasing with the degree of unsaturation but decreasing with fatty acid chain length. NO_x emissions of hydrogenated FAMEs derived from soybean oil is lower than from conventional diesel.[70]

Oxidation stability also depends upon the degree of unsaturation of fatty acid chains within the oil feedstock, since double bonds are prone to oxidation. Biodiesel produced from feedstocks containing linoleic (C18, two C═C double bonds) and linolenic acid (C18, three C═C double bonds), with one or two bis-allylic positions, are highly susceptible to oxidation. The relative rates of oxidation for linoleates and linolenates are respectively 41 and 98 times higher than that of the monounsaturated oleate.[71] The viscosity of biodiesel also increases with chain length and saturation of fatty acids within the feedstock,[72] influencing the fuel lubricity and flow properties. Low viscosity biodiesel can be obtained from low molecular weight triglycerides, however such biodiesel cannot be used directly as a fuel due to its poor cold temperature flow properties. The kinematic viscosities of the two most common biodiesels are 4.0–4.1 mm^2 s^{-1} from soybean oil and 4.4 mm^2 s^{-1} from rapeseed oil. The lubricity of biodiesel increases with chain length, and the presence of double bonds and alcohol groups. Hence, monoglycerides and trace glycerol increase biodiesel lubricity. The high lubricity of biodiesel can be utilised through blending with conventional, low-sulfur diesel to improve overall fuel lubricity.[73] Cold point (CP) and pour point (PP) determine the flow properties of biodiesel, and also depend on the fatty acid composition of the feedstock. CP is the temperature at which a fuel begins to solidify, and PP is the temperature at which the fuel can no longer flow. For conventional diesel, CP and PP values are −16 °C and −27 °C respectively. Biodiesel derived from soybean possesses CP and PP values of around 0 °C to −2 °C, while the CP for rapeseed oil-derived biodiesel is −3 °C. These values are very high in comparison to conventional diesel, rendering biodiesel ill-suited for cold countries.[70] Other common feedstocks, such as palm oil, jatropha oil, animal fat and waste cooking oil have even higher CP values of around 15 °C. In contrast, biodiesel derived from *cuphea* oil enriched with saturated, medium-chain C8–C14 fatty acids exhibits improved properties including a lower CP of −9 to −10 °C,[74] comparable to conventional diesel. Genetic engineering of the parent plants or microalgae offers a route to optimise the fatty acid composition of feedstock oils to deliver fuels with the desired physicochemical properties.[75]

3. Solid base catalysed biodiesel synthesis

Base catalysts are generally more active than acids in transesterification, and hence are particularly suitable for high purity oils with low FFA content. Biodiesel synthesis using a solid base catalyst in continuous flow, packed bed arrangement would facilitate both catalyst separation and co-production of high purity glycerol, thereby reducing production costs and enabling catalyst re-use. Diverse solid base catalysts are known, notably alkali or alkaline earth oxides, supported alkali metals, basic zeolites and clays such as hydrotalcites, and immobilised organic bases.[76]

3.1 Alkaline earth oxides

Basicity in alkaline earth oxides is believed to arise from M^{2+}–O^{2-} ion pairs present in different coordination environments.[77] The strongest base sites occur at low coordination defect, corner and edge sites, or on high Miller index surfaces. Such classic heterogeneous base catalysts have been extensively tested for TAG transesterification[78] and there are numerous reports on commercial and microcrystalline CaO applied to

Open Access Article. Published on 24 June 2014. Downloaded on 1/3/2025 11:41:55 PM.
This article is licensed under a Creative Commons Attribution 3.0 Unported Licence.

rapeseed, sunflower or vegetable oil transesterification with methanol.[79,80] Promising results have been obtained, with 97% oil conversion achieved at 75 °C,[80] however concern remains over Ca^{2+} leaching under reaction conditions and associated homogeneous catalytic contributions,[81] a common problem encountered in metal catalysed biodiesel production which hampers commercialisation.[82] While Ca and Mg are the more widely used alkaline earth metals in solid base catalysis, strontium oxides have also found application in biodiesel production. Pure strontium oxide possesses the highest base site density of the alkali earth oxides as determined by CO_2 temperature programmed desorption (TPD),[83] and a comparable base strength to that of BaO ($26.5 < H_-$). Despite the lower surface area of SrO compared to Mg and Ca oxides (19, 14 and 3 $m^2\ g^{-1}$ respectively), it showed the highest activity for hempseed oil transesterification, although it is questionable whether such low area/highly soluble materials could ever be commercially viable.

Alkali-doped CaO and MgO have also been investigated for TAG transesterification,[84–86] with their enhanced basicity attributed to the genesis of O^- centres following the replacement of M^+ for M^{2+} and associated charge imbalance and concomitant defect generation. In the case of Li-doped CaO, the electronic structure of surface lithium ions (as probed by XPS) evolves discontinuously as a function of concentration and phase. Maximal activity was observed upon formation of a saturated Li^+ monolayer, with the phase to bulk-like $LiNO_3$ at higher loadings suppressing TAG conversion coincident with loss of strong base sites.[86] However, leaching of alkali promoters remains problematic.[87]

It is widely accepted that the catalytic activity of alkaline earth oxide catalysts is very sensitive to their preparation, and corresponding surface morphology and/or defect density. For example, Parvulescu and Richards demonstrated the impact of the different MgO crystal facets upon the transesterification of sunflower oil by comparing nanoparticles[88] *versus* (111) terminated nanosheets.[89] Chemical titration revealed that both morphologies possess two types of base sites, with the nanosheets exhibiting well-defined, medium-strong basicity consistent with their uniform exposed facets and which confer higher FAME yields during sunflower oil transesterification (albeit scale-up of the nanosheet catalyst synthesis may be costly and non-trivial). Subsequent synthesis, screening and spectroscopic characterisation of a family of size-/shape-controlled MgO nanoparticles prepared *via* a hydrothermal synthesis, revealed small (<8 nm) particles terminate in high coordination (100) facets, and exhibit both weak polarisability and poor activity in tributyrin transesterification with methanol.[90] Calcination drives restructuring and sintering to expose lower coordination stepped (111) and (110) surface planes, which are more polarisable and exhibit much higher transesterification activities under mild conditions. A direct correlation was therefore observed between the surface electronic structure and associated catalytic activity, revealing a pronounced structural preference for (110) and (111) facets (Fig. 1). *In situ* aberration corrected-transmission electron microscopy and XPS implicates

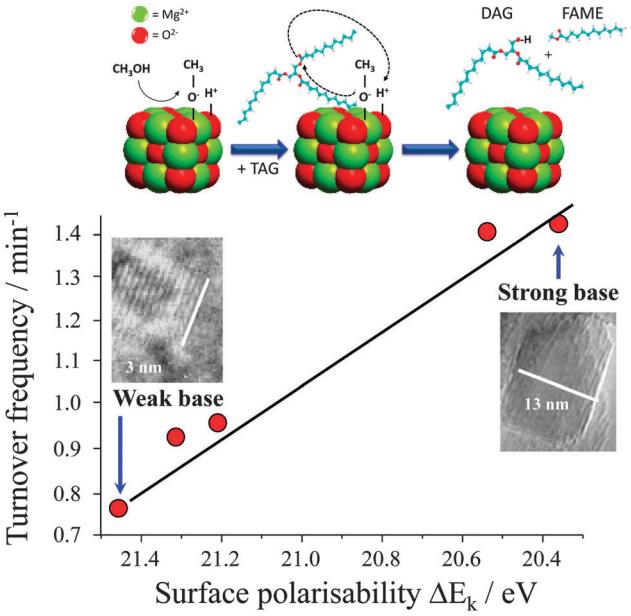

Fig. 1 Relationship between surface polarisability of MgO nanocrystals and their turnover frequency towards tributyrin transesterifcation. Adapted from ref. 90 with permission from The Royal Society of Chemistry.

coplanar anion vacancies as the active sites in tributyrin transesterification with the density of surface defects predicting activity.[90,91]

Cesium doping *via* co-precipitation under supercritical conditions confers even greater activity towards tributyrin transesterification with methanol,[85] due to the genesis of additional, and stronger, base sites associated with a new ordered mixed oxide phase which EXAFS analysis recently identified as $Cs_2Mg(CO_3)_2(H_2O)_4$,[92] resulting in superior performance compared with MgO and even homogeneous Cs_2CO_3 catalysts (Fig. 2). Unfortunately, surface carbon deposition and loss of this high activity $Cs_2Mg(CO_3)_2(H_2O)_4$ phase due to partial Cs dissolution results in on-stream deactivation of Cs-doped MgO, although recalcination could help to regenerate activity.

Alkaline earth metal oxides may be incorporated into metal oxides to form composite oxides[93] which are also suitable as solid base catalysts for biodiesel production. The activity of such composites is similar to that of the parent alkaline earth (typically CaO), but they exhibit greater stability and are less prone to dissolution, facilitating separation from the reaction media. Calcination temperature strongly influences the resulting catalytic activity towards transesterification. For example, a Ca–Al composite oxide containing $Ca_{12}Al_{14}O_{33}$ and CaO thermally processed between 120 °C and 1000 °C showed maximal activity after a 600 °C treatment due to changes in specific surface area and crystallinity. CaO was only observed in samples prepared >600 °C, accompanied by the formation of crystalline $Ca_{12}Al_{14}O_{33}$. Synergy between these two phases greatly improved the transesterification activity, however calcination at temperatures significantly above 600 °C induced crystallite sintering and concomitant loss of surface area and activity. Unfortunately the catalyst synthesis employed sodium

Open Access Article. Published on 24 June 2014. Downloaded on 1/3/2025 11:41:55 PM.
This article is licensed under a Creative Commons Attribution 3.0 Unported Licence.

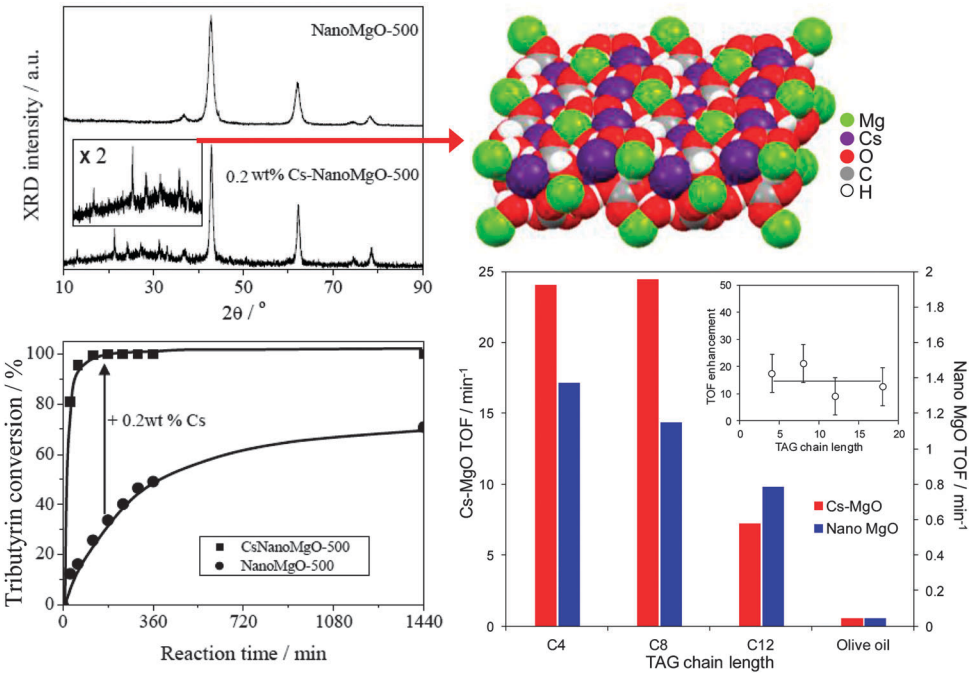

Fig. 2 Formation of crystalline $Cs_2Mg(CO_3)_2(H_2O)_4$ phase within co-precipitated Cs-doped MgO and resulting synergy in the transesterification of short and long chain TAGs with methanol compared with undoped nanocrystalline MgO. Adapted from ref. 85 with kind permission from Springer Science and Business Media and ref. 92 with permission from John Wiley and Sons.

precursors, hence alkali contamination of these catalysts cannot be discounted, and which in any event were employed at high loadings (6 wt%) and without recycle tests.

Calcium also forms a mixed oxide with MoO_3.[94] Supporting both oxides on SBA-15 mesoporous silica afforded a transesterification catalyst with improved stability relative to CaO due the presence of acidic MoO_3 sites on the SBA-15. The impact of Ca : Mo ratio and calcination temperatures was explored, with a Ca : Mo ratio of 6 : 1 maximising activity for soybean oil conversion, boosting FAME yields from 48 to 83% over extremely long reaction times in excess of 50 h. Raising the calcination temperature from 350 °C to 550 °C induced CaO and MoO_3 crystallisation, with a corresponding rise in activity; higher temperature calcination did not promote further crystallisation and was not beneficial for transesterification.

Alkaline earth oxides may be used to support acidic or amphoteric materials to form materials with mixed acid–base character. Transesterification of soybean oil over CaO supported SnO_2 prepared *via* impregnation was highly dependent on calcination temperature and the Ca : Sn ratio.[95] The interaction between acidic SnO_2 and basic CaO resulted in a highly SnO_2 phase and associated active sites. Calcination above 350 °C was required to initiate decomposition of the Ca precursor, with temperatures >650 °C driving complete conversion to Ca oxides. Optimal performance was obtained for high calcination temperatures, which maximised the CaO content. Further heating again led to particle sintering/agglomeration and decreased reactivity. Supported CuO can also produce biodiesel from hempseed oil,[83] with 10 wt% CuO/SrO offering 20% higher FAME yields under optimised conditions than other alkaline earth oxides. The CuO could also undergo chemical reduction during transesterification to form an active catalyst for the selective hydrogenation of polyunsaturated hydrocarbons for further biodiesel upgrading. It should be noted that the catalyst loadings employed in this study of 4–12 wt% would likely prove prohibitive in any commercial process, and that small but significant (29 ppm) quantities of leached Ca may have contributed to the observed performance.

Composites of Sr and Al were prepared by Farzaneh *et al.* and evaluated for soybean oil transesterification with methanol.[96] The dominant crystalline phase was $Sr_3Al_2O_6$, giving rise to medium and high strength base sites with corresponding CO_2 desorption peak maxima of 388 °C and 747 °C respectively. The Sr–Al oxide also possessed a higher density of base sites compared to solid bases such as CaO/Al_2O_3, reflected in an eight-fold higher CO_2 adsorption capacity. These superior base properties enhanced the activity of the strontium composite for soybean transesterification to FAMEs, resulting in comparable conversions at a lower catalyst loading and shorter reaction time than for a MgAl hydrotalcite and CaO/Al_2O_3. While oil conversions fell noticeably with repeated re-use, there was no evidence of alkaline earth dissolution, and the resulting biodiesel fuel met ASTM and EN standards.

3.2 Alkali doped materials

As shown in Fig. 1, lithium doped CaO can enhance tributyrin transesterification. Li doping has also been exploited over SiO_2, wherein 800 °C calcination results in a lithium orthosilicate solid base catalyst, Li_4SiO_4.[97] Although the basic strength of Li_4SiO_4, determined by Hammett indicators, was less than that

Open Access Article. Published on 24 June 2014. Downloaded on 1/3/2025 11:41:55 PM.
This article is licensed under a Creative Commons Attribution 3.0 Unported Licence.

of CaO, both materials exhibited similar initial activity towards soybean transesterification, with the lithium orthosilicate more stable and maintaining activity after prolonged exposure to air, in contrast to CaO. The superior stability of the Li_4SiO_4 catalyst was further demonstrated by its water and carbon dioxide tolerance, both of which poison conventional alkaline earth catalysts.

Sodium silicate, Na_2SiO_3, is also active for biodiesel production from rapeseed and *jatropha* oils under both conventional[98] and microwave assisted conditions,[99] with a 98% FAME yield after one hour reaction under mild conditions. Although this catalyst displayed good recyclability, TAG conversions fell steadily to <60% after four re-uses, attributed to water adsorption and Si–O–Si bond cleavage and sodium leaching.[98] The same catalyst was evaluated using microwave heating for only five minutes at a range of powers between 100–500 W (Fig. 3).[99] At low power only 18% rapeseed oil conversion was obtained. Higher powers heated the reaction mixture (to ~175 C for 400 W) in turn boosting FAME yields from both oils to ~90%, highlighting the use of microwave heating to accelerate biodiesel production. Recycle studies again showed slow *in situ* deactivation due to particle agglomeration, water adsorption of water, and associated loss of basicity due to sodium leaching into methanol during both transesterification and washing procedures between recycles. Despite some recent successes in the scale-up of microwave-assisted (homogeneously catalysed) biodiesel production (see Section 6),[28,100] it remains unlikely that such heating solutions can deliver the high throughput demanded for commercial processes.

Activated carbon can be used as an amphoteric support for basic alkaline metal salts such as K_2CO_3,[101] which is known to be an active homogeneous catalyst for oil transesterification and biodiesel production.[102] A study of K_2CO_3 supported over a range of support materials, such as MgO, activated carbon and SiO_2, demonstrated that K_2CO_3 on basic carriers gave higher activity for rapeseed oil transesterification than when using acidic carriers (unsurprisingly due to self-neutralisation!).[102] K_2CO_3/MgO was shown to be highly stable, with spent catalysts showing minimal loss of performance over six re-uses (though requiring 400 °C reactivation between cycles), and exhibiting negligible structural changes or potassium leaching. Kraft lignin is a low cost, renewable by-product of the Kraft wood pulping process, and possesses high carbon and low ash content and is therefore a popular precursor for activated carbons. Li *et al.* used K_2CO_3 in a one-pot method to prepare activated carbon and transform this into a solid base catalyst, namely K_2CO_3 on Kraft Lignin activated carbon (LKC), for biodiesel production.[101] Thermal activation had a significant impact on the resulting catalytic activity, with higher calcination temperatures increasing the surface area and pore volume 100-fold and hence FAME production, however temperatures above 800 °C induced K_2CO_3 decomposition and poorer performance. Optimal reaction conditions of 65 °C, 3 wt% loading and a K/KLC ratio of 0.6, enabled a 98% FAME yield from rapeseed oil transesterification, which fell to 82% after four recycles as a result of progressive particle agglomeration and potassium leaching into the biodiesel. Wu *et al.* supported a range of potassium salts on mesoporous silicas for use as solid base biodiesel catalysts.[103] A K_2SiO_3 impregnated catalyst proved superior to K_2CO_3 and KAc impregnated catalysts due to its higher base site density (1.94 *versus* 1.81 and 1.72 mmol g^{-1} respectively). Aluminium addition to the SBA-15 framework improved the morphology, increasing the surface area and pore volume, and CO_2 desorption temperature indicative of a

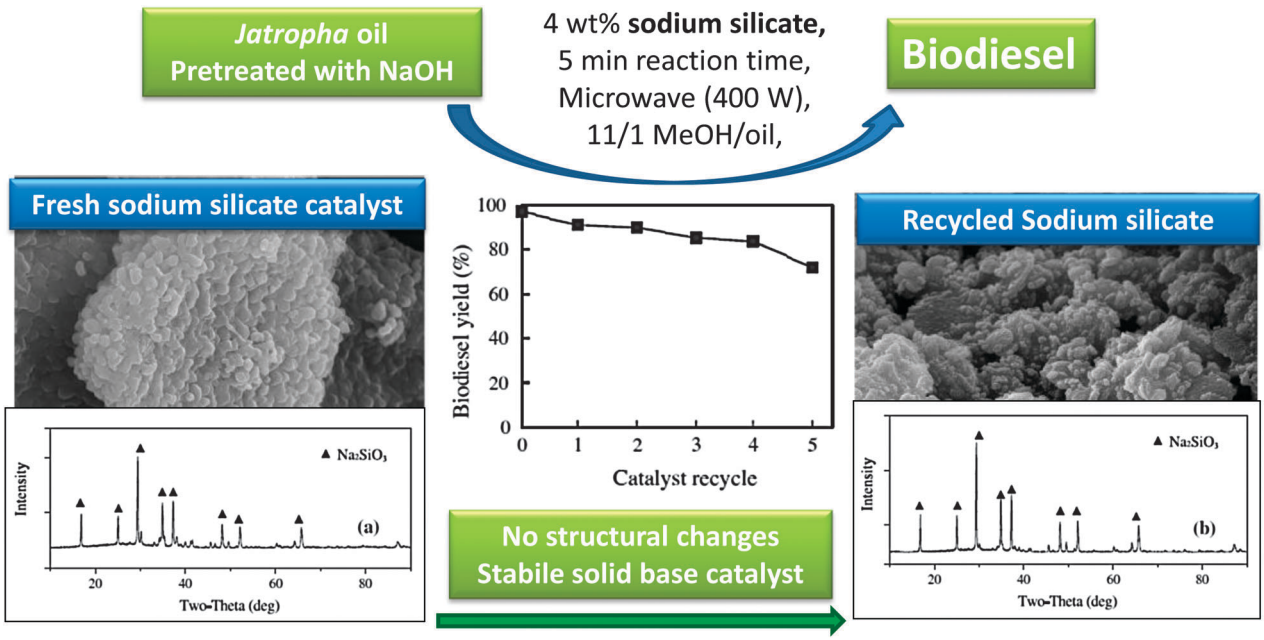

Fig. 3 Demonstration of the structural stability and catalytic activity of sodium silicate as a solid base for biodiesel production. Adapted from ref. 99. Copyright (2014), with permission from Elsevier.

Open Access Article. Published on 24 June 2014. Downloaded on 1/3/2025 11:41:55 PM.
This article is licensed under a Creative Commons Attribution 3.0 Unported Licence.

more strongly basic support; this observation is rather counter-intuitive, since Al-doping of SBA-15 is usually employed to promote the formation of Brönsted and Lewis acid sites of moderate acidity.[104] A 30% K_2SiO_3/AlSBA-15 catalyst was used for the transesterification of Jatropha oil with MeOH at 60 °C, giving 95% conversion for a relatively low MeOH/oil molar ratio of 9 : 1. This catalyst was recycled five times with only a 6% drop in conversion, but the filtered catalyst required regenerative washing with a methanol–*n*-hexane mixture and re-calcination to avoid a significant drop in FAME yield to 47% after the fifth recycle. The magnitude of this activity loss indicates significant K leaching. In a related study, Xie *et al.* immobilised tetraalkylammonium hydroxides onto SBA-15 for soybean oil transesterification.[105] The resulting SBA-15-pr-NR_3OH catalyst gave 99% conversion to FAMEs under methanol reflux. Covalent linking of the tetraalkylammonium hydroxide to the silica surface prevented *in situ* leaching, resulting in only a 1% fall in FAME yield after five recycles and appears a promising methodology for biodiesel production at mild-moderate temperatures under which the covalently linked propyl backbone is thermally stable.

Despite its importance in the context of second generation biofuels, waste biomass has been less extensively investigated in catalyst preparation. Most such studies have focused on the synthesis of carbonaceous solid acid catalysts[2,106–109] as discussed later. In contrast, rice husk ash modified with Li *via* a simple solid state preparative route, has been exploited as a solid base catalyst by for soybean oil transesterification with methanol.[106] These materials exhibited high basicity ($H_- > 15.0$), comparable to that of CaO, and consequent high activity, but superior air stability than CaO which deactivated due to hydration; the Li rice husk catalyst showed only a modest drop in oil conversion from 97% to 82% upon re-use. As with any material derived from a biogenic source the question of compositional variability arises, particularly in regard to residual heavy metals in the ash, which is likely to hamper catalyst reproducibility.[110]

3.3 Transition metal oxides

Solid bases usually afford higher rates of transesterification than solid acids, hence a range of transition metal oxides of varying Lewis base character have been explored in biodiesel production. MnO and TiO are mild bases with good activity for biodiesel production,[111] and have been applied for the simultaneous transesterification of triglycerides and esterification of FFAs under continuous flow conditions using low grade feedstocks with high fatty acid contents (up to 15%). Soap formation, caused by leaching of metal from the catalyst surface under high FFA concentrations, was an order of magnitude less than that observed with conventional homogeneous base catalysts. Unfortunately, this study did not characterise the Mn or Ti oxidation state in either fresh or spent materials to confirm the nature of any catalytic centre. Zirconium has also been shown to activate and stabilise solid base catalysts for biodiesel production.[101,112,113] Mixed oxides of CaO and ZrO_2 prepared *via* co-precipitation showed increased surface area and stability with increasing Zr : Ca ratios (Fig. 4). However, the transesterification activity remained dependent upon the Ca content, decreasing at lower CaO loadings.[112] Sodium zirconate, a potential CO_2 adsorbent,[84,114] has shown promise in biodiesel production,[113] with 98% conversion of soybean oil to FAME after 3 h at 65 °C. Deactivation observed upon repeated decanting and recycling was attributed to surface poisoning, with methanol washing between cycles facilitating 84% conversion after five recycles. This material's affinity for carbon dioxide and large crystallite size/low surface area (~1 m^2 g^{-1}) may render it air-sensitive and prone to further sintering. Zirconia was employed as a support for a range of sodium-containing bases, such as NaOH, NaH_2PO_4, $C_4H_5O_6Na$ (monosodium tartrate) and potassium

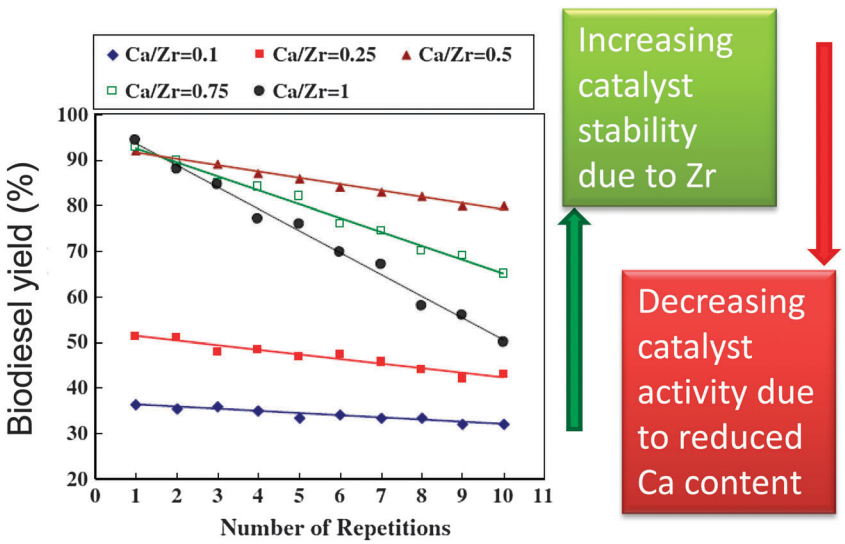

Fig. 4 Effect of Zr-doping on CaO solid base catalysts for biodiesel production. Adapted from reference 112. Copyright (2012), with permission from Elsevier.

Open Access Article. Published on 24 June 2014. Downloaded on 1/3/2025 11:41:55 PM.
This article is licensed under a Creative Commons Attribution 3.0 Unported Licence.

sodium tartrate were doped on ZrO_2 to prepare a series of catalysts with varying basic strength and total basicity for the microwave assisted transesterification of soybean oil with methanol.[101] Catalytic activity was dependent upon basicity, increasing at higher Na : Zr ratios. The potassium sodium tartrate doped zirconia exhibited the strongest basicity and highest conversions, reaching 54% for Na : Zr = 1 and a 1 : 10 catalyst : soybean oil mass ratio at 60 °C under 600 W microwave power. Increasing the Na : Zr ratio to 2 improved conversion to 92%. Optimal conversions were obtained for catalysts calcined at 600 °C, possibly due to tartrate decomposition at higher temperatures, although this catalyst was recyclable *via* filtration and re-calcination.

Porosity was introduced to a titania-based catalyst through the construction of sodium titanate nanotubes as solid base catalysts for soybean oil transesterification with methanol.[115] The catalyst exhibited a range of active sites of varying basicity, however the high sodium content (10 wt%) is a cause for concern due to the high probability of leaching *in situ* and associated homogeneous chemistry. The pore distribution was bimodal, consisting of 3 nm wide tubular mesopores and ~40 nm voids between the aggregated nanotubes. Biodiesel yields of >97% were obtained for 1–2 wt% of catalyst at 65 °C. However, a large excess of methanol to oil was required (40 : 1 molar ratio), and while this material could be re-used several times, it was less active than that of CaO and MgO lacking such a nanoporous architecture.

3.4 Hydrotalcites

Hydrotalcites are another class of solid base catalysts that have attracted attention because of their high activity and robustness in the presence of water.[116,117] Hydrotalcites ($[M(II)_{1-x}M(III)_x(OH)_2]^{x+}(A^{n-}{}_{x/n})\cdot mH_2O$) adopt a layered double hydroxide structure with brucite-like ($Mg(OH)_2$) hydroxide sheets containing octahedrally coordinated M^{2+} and M^{3+} cations, separated by interlayer A^{n-} anions to balance the overall charge,[118] and are conventionally synthesised *via* co-precipitation from their nitrates using alkalis as both pH regulators and a carbonate source. Mg–Al hydrotalcites have been applied to TAG transesterification of poor and high quality oil feeds,[119] such as refined and acidic cottonseed oil (possessing 9.5 wt% FFA) and animal fat feed (45 wt% water), delivering 99% conversion within 3 h at 200 °C. It is important to note that many catalytic studies employing hydrotalcites for transesterification are suspect due to their use of Na or K hydroxide/carbonate solutions to precipitate the hydrotalcite phase. Complete removal of alkali residues from the resulting hydrotalcites is inherently difficult, resulting in ill-defined homogeneous contributions to catalysis arising from leached Na or K.[120,121] This problem has been overcome by the development of alkali-free precipitation routes employing NH_3OH and NH_3CO_3, which offer well-defined, thermally activated and rehydrated Mg–Al hydrotalcites with compositions spanning x = 0.25–0.55.[116] Spectroscopic measurements reveal that increasing the Mg : Al ratio enables systematic enhancement of the surface charge and accompanying base strength, with a concomitant increase in the rate of

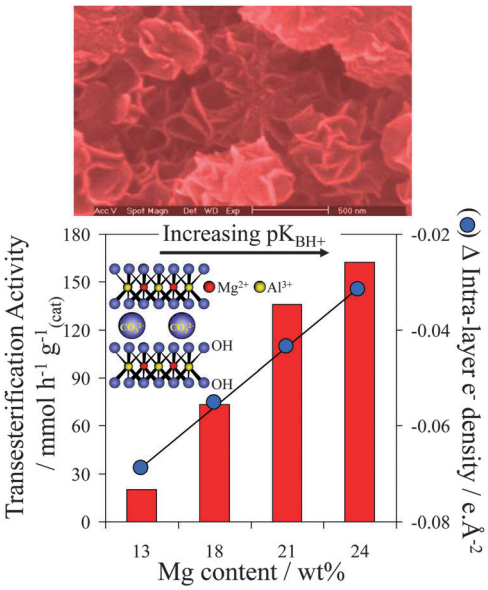

Fig. 5 Impact of Mg:Al hydrotalcite surface basicity on their activity towards tributyrin transesterification. Adapted from ref. 117. Copyright (2005), with permission from Elsevier.

tributyrin transesterification under mild reaction conditions (Fig. 5). Despite their high intrinsic activity, one limitation of co-precipitated pure hydrotalcites is their low surface areas, although delamination[122,123] and grafting[124] methodologies offer avenues to circumvent this.

Since conventionally-prepared hydrotalcites are microporous, they are poorly suited to transesterification of bulky C_{16}–C_{18} TAGs which are the principal components of bio-oils. One solution has therefore been to utilise catalysts possessing a bimodal pore distribution, wherein micropores provide a high surface density of base sites while a complementary meso- or macropore network affords rapid transport of TAGs from the bulk reaction media to these active sites, and removal of FAME and glycerol products back out from the porous catalyst. Ordered, hierarchical materials possessing such bimodal pore architectures can be prepared by combining hard and soft templating approaches, exemplified by the methodology developed by Géraud and co-workers, wherein co-precipitation of the divalent and trivalent metal cations occurs within the interstices of an infiltrated polystyrene (PS) colloidal crystal.[125,126] This approach has been adopted to incorporate macroporosity into an alkali-free Mg–Al hydrotalcite, and thus create a hierarchical macroporous–microporous hydrotalcite solid base catalyst.[127] The resulting macropores act as rapid access conduits to transport heavy TAG oil components to active base sites present at the surface of (high aspect ratio) hydrotalcite nanocrystallites, thereby promoting triolein transesterification compared with that achievable over a Mg–Al microporous hydrotalcite of identical chemical composition (Fig. 6). Spiking experiments confirm that transesterification of the bulky C_{18} triolein by the hierarchical hydrotalcite catalyst is less hindered by reactively-formed glycerol than when using a conventional microporous hydrotalcite (wherein glycerol completely suppresses biodiesel production). In contrast

Open Access Article. Published on 24 June 2014. Downloaded on 1/3/2025 11:41:55 PM.
This article is licensed under a Creative Commons Attribution 3.0 Unported Licence.

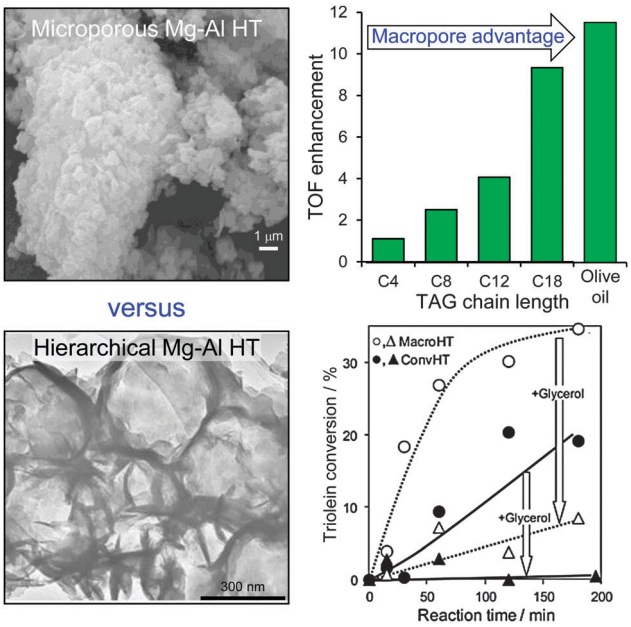

Fig. 6 Superior catalytic performance of a hierarchical macroporous–microporous Mg–Al hydrotalcite solid base catalyst for TAG transesterification to biodiesel *versus* a conventional microporous analogue. Adapted from ref. 128 with permission from The Royal Society of Chemistry.

the more mobile model C_4 TAG, trubutyrin possesses an infinite dilution diffusion coefficient of 0.074 $cm^2\ s^{-1}$ in methanol *versus* 0.037 $cm^2\ s^{-1}$ for the triolein in methanol. Future scalability of such hierarchical catalysts will require either improved extraction protocols to enable re-use of the colloidal PS template, or the development of alternative polymeric templates derived from sustainable resources, such as polylactic or poly(lactide-*co*-glycolide) nanospheres.[128]

In terms of sustainability, it is important to find low cost routes to the synthesis of solid base catalysts that employ earth abundant elements. Dolomitic rock, comprising alternating $Mg(CO_3)$–$Ca(CO_3)$ layers, is structurally very similar to calcite ($CaCO_3$), with a high natural abundance and low toxicity, and in the UK is sourced from quarries working Permian dolomites in Durham, South Yorkshire and Derbyshire.[129] In addition to uses in agriculture and construction, dolomite finds industrial applications in iron and steel production, glass manufacturing and as fillers in plastics, paints, rubbers, adhesives and sealants. Catalytic applications for powdered, dolomitic rock offer the potential to further valorise this readily available waste mineral, and indeed dolomite has shown promise in biomass gasification[130] as a cheap, disposable and naturally occurring material that significantly reduces the tar content of gaseous products from gasifiers. Dolomite has also been investigated as a solid base catalyst in biodiesel synthesis,[131] wherein fresh dolomitic rock comprised approximately 77% dolomite and 23% magnesian calcite. High temperature calcination induced Mg surface segregation, resulting in MgO nanocrystals dispersed over $CaO/(OH)_2$ particles, while the attendant loss of CO_2 increases both the surface area and basicity. The resulting calcined dolomite proved an effective catalyst for the transesterification of C_4, C_8 and TAGs with methanol and longer chain C_{16-18} components present within olive oil, with TOFs for tributyrin conversion to methyl butanoate the highest reported for any solid base. The slower transesterification rates for bulkier TAGs were attributed to diffusion limitations in their access to base sites. Calcined dolomite has also shown promise in the transesterification of canola oil with methanol, achieving 92% FAME after 3 h reaction with 3 wt% catalyst.[132]

Doping of (calcined) Malaysian dolomite with ZnO and SnO_2 resulted in respective three- and four-fold increases in the catalyst surface area and active base density, and a concomitant rise in base strength.[133] The SnO_2 doped dolomite gave >99.9% conversion under optimised conditions with a low methanol : oil molar ratio and catalyst loading.

Other waste materials employed for biodiesel production include waste water scale (obtained from residential kitchens in China), which upon 1000 °C calcination yielded a solid base material mixture of CaO, MgO, Fe_2O_3, Al_2O_3, and SiO_2 as a stable and active catalyst for soybean transesterification with methanol.[134] This composition is similar to that of Red Mud mineral waste, recently shown to be an active ketonisation catalyst.[135,136] This waste to resource approach of catalyst design is highly desirable in terms of green credentials and the biofuel ideology.

In summary, a host of inorganic solid base catalysts have been developed for the low temperature transesterification of triglyceride components of bio-oil feedstocks, offering activities far superior to those achieved *via* alternative solid acid catalysts to date. However, leaching of alkali and alkaline-earth elements and associated catalyst recycling remains a challenge, while improved resilience to water and fatty acid impurities in plant, algal and waste oil feedstocks is required in order to eliminate additional esterification pre-treatments.

4. Solid acid catalysed biodiesel synthesis

A wide range of inorganic and polymeric solid acids are commercially available, however their application for the transesterification of oils into biodiesel has only been recently explored, in part reflecting their lower activity compared with base-catalysed routes,[32] in turn necessitating higher reaction temperatures to deliver suitable conversions. Despite their generally poorer activity, solid acids have the advantage that they are less sensitive to FFA contaminants then their solid base analogues, and hence can operate with unrefined feedstocks containing high acid contents.[32] In contrast to solid bases, which require feedstock pretreatment to remove these fatty acid impurities, solid acids are able to esterify FFAs through to FAME in parallel with transesterification of major TAG components, without saponification, and hence enable a reduction in the number of processing steps to biodiesel.[137–139]

4.1 Mesoporous silicas

Mesoporous silicas from the SBA family[140] have been examined for biodiesel synthesis, and include materials grafted with

Open Access Article. Published on 24 June 2014. Downloaded on 1/3/2025 11:41:55 PM.
This article is licensed under a Creative Commons Attribution 3.0 Unported Licence.

sulfonic acid groups[141,142] or SO_4/ZrO_2 surface coatings.[143] Phenyl and propyl sulfonic acid SBA-15 catalysts are particularly attractive materials with activities comparable to Nafion and Amberlyst resins in palmitic acid esterification.[144] Phenylsulfonic acid functionalised silica are reportedly more active than their corresponding propyl analogues, in line with their respective acid strengths, but are more difficult to prepare. Unfortunately, conventionally synthesised sulfonic acid-functionalised SBA-15 silicas possess pore sizes below ~6 nm and long, isolated parallel channels, and suffer correspondingly slow in-pore diffusion and catalytic turnover in FFA esterification. However, poragens such as trimethylbenzene,[145] triethylbenzene and triisopropylbenzene[146] can induce swelling of the Pluronic P123 micelles used to produce SBA-15, enabling ordered mesoporous silicas with diameters spanning 5–30 nm. This methodology was recently applied to prepare a range of large pore SBA-15 materials employing trimethylbenzene as the poragen, resulting in the formation of highly-ordered periodic mesostructures with pore diameters of ~6, 8 and 14 nm.[127] These silicas were subsequently functionalised by mercaptopropyl trimethoxysilane (MPTS) and oxidised with H_2O_2 to yield expanded $PrSO_3$-SBA-15 catalysts which were effective in both palmitic acid esterification with methanol and tricaprylin and triolein transesterification with methanol under mild conditions. For both reactions, turnover frequencies dramatically increased with pore diameter, and all sulfonic acid heterogeneous catalysts significantly outperformed a commercial Amberlyst resin. These rate enhancements are attributed to superior mass-transport of the bulky free fatty acid and triglycerides within the expanded $PrSO_3$-SBA-15. Similar observations have been made over poly(styrenesulfonic acid)-functionalised, ultra-large pore SBA-15 in the esterification of oleic acid with butanol.[147] Mesopore expansion accelerates reactant/product diffusion to/from active sites, but there are limits to the extent to which this can be achieved without concomitant loss of pore ordering, which hampers mesoscopic modelling.[148]

The two dimensional, micron-length channels characteristic of the SBA-15 *p6mm* structure are known to hamper rapid molecular exchange with the bulk reaction media, and hence three dimensional interconnected channels associated with the $Ia\bar{3}d$ structure of KIT-6 mesoporous silica offer one solution to improving the in-pore accessibility of sulfonic acid sites. Superior molecular transport within the interconnected cubic structure of KIT-6 has been shown to facilitate biomolecule immobilisation.[149] This diversity of mesoporous silica architectures enabled the impact of pore connectivity upon FFA esterification to be quantified.[150] A family of pore-expanded propylsulfonic acid KIT-6 analogues, $PrSO_3H$-KIT-6, prepared *via* MPTS grafting and subsequent oxidation, have been screened for FFA esterification with methanol under mild conditions. Such a conventionally-prepared material exhibited 40 and 70% TOF enhancements for propanoic and hexanoic acid esterification respectively over an analogous $PrSO_3H$-SBA-15 catalyst of comparable (5 nm) pore diameter, attributed to faster mesopore diffusion. However, pore accessibility remained rate-limiting for esterification of the longer chain lauric and palmitic acids. Pore expansion of the KIT-6 mesopores up to 7 nm *via* hydrothermal ageing doubled the resulting TOFs for lauric and palmitic acid esterification with respect to an unexpanded $PrSO_3H$-SBA-15 (Fig. 7). It should be noted that the absolute conversions of FFAs over such tailored, inorganic solid acid catalysts remain significantly lower than those for commercial polymer alternatives which possess superior acid site densities (*e.g.* 4.7 mmol g^{-1} for Amberlyst-15[151] *versus* <1 mmol g^{-1} for $PrSO_3H$-SBA-15 and $PrSO_3H$-KIT-6[150]).

Propylsulfonic acid functionalised SBA-15 (SBA-15-$PrSO_3H$) has also been evaluated for oleic acid esterification with methanol,[152] showing good stability in boiling water, with the mesopore structure allowing facile diffusion of the acid to active sites. This catalyst exhibited similar activity to phenylethylsulfonic acid functionalised silica gel, and was superior to dry Amberlyst-15, reflecting the higher surface area and pore volume of the SBA-15-$PrSO_3H$ relative to the more strongly acidic phenylethyl mesoporous silica. The SBA-15-$PrSO_3H$ could be recycled by simple ethanol washing and drying at 80 °C, and maintained an esterification rate of 2.2 mmol min^{-1} g_{cat}^{-1}. Simultaneous esterification and transesterification of vegetable

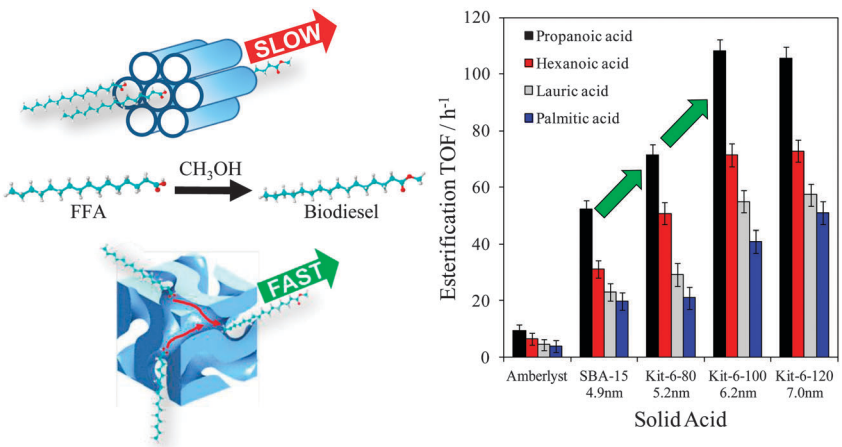

Fig. 7 Superior performance of interconnected, mesoporous propylsulfonic acid KIT-6 catalysts for biodiesel synthesis *via* free fatty acid esterification with methanol *versus* non-interconnected mesoporous SBA-15 analogue. Adapted from ref. 151. Copyright 2012 American Chemical Society.

Open Access Article. Published on 24 June 2014. Downloaded on 1/3/2025 11:41:55 PM.
This article is licensed under a Creative Commons Attribution 3.0 Unported Licence.

oils with methanol has performed with Ti-doped SBA-15.[153] A range of oils including soybean, rapeseed, crude palm, waste cooking oil and crude Jatropha oil (CJO), and palm fatty acid distillates were successfully converted to biodiesel by the Ti-SBA-15 catalyst at 200 °C. The mesoporous framework gave improved accessibility to the weakly Lewis acidic Ti^{4+} sites, affording higher activity than microporous titanosilicate and TiO_2 supports. The Ti-SBA-15 was tolerant of common oil impurities, performing well in the presence of 5 wt% water or 30 wt% FFA. High catalyst loadings of 15 wt% relative to CJO permitted recycling without loss in conversion, although catalyst regeneration between recycles necessitated washing with acetone and subsequent 500 °C calcination.

Most solid acid catalysts employed in biodiesel synthesis are microporous or mesoporous,[32,34,154] properties which the preceding sections highlights are not desirable for accommodating sterically-challenging C_{16}–C_{18} TAGs or FFAs for biodiesel synthesis. Incorporation of secondary mesoporosity into a microporous H-β-zeolite to create a hierarchical solid acid significantly accelerated microalgae oil esterification with methanol by lowering diffusion barriers.[155] Templated mesoporous solids are widely used as catalyst supports,[156,157] with SBA-15 silica popular candidates for reactions pertinent to biodiesel synthesis as described above.[142,144,158] However, such surfactant-templated supports possessing long, isolated parallel and narrow channels to not afford efficient in-pore diffusion of bio-oil feedstocks, with resultant poor catalytic turnover. Further improvements in pore architecture are hence required to optimise mass-transport of heavier, bulky TAGs and FFAs common in plant and algal oils. Simulations demonstrate that in the Knudsen diffusion regime,[159] where reactants/products are able to diffuse enter/exit mesopores but experience moderate diffusion limitations, hierarchical pore structures may significantly improve catalyst activity. Materials with interpenetrating, bimodal meso-macropore networks have been prepared using microemulsion[160] or co-surfactant[161] templating routes and are particularly attractive for liquid phase, flow reactors wherein rapid pore diffusion is required. Liquid crystalline (soft) and colloidal polystyrene nanospheres (hard) templating methods have been combined to create highly organised, macro-mesoporous aluminas[162] and 'SBA-15 like' silicas[163] (Scheme 4), in which both macro- and mesopore diameters can be independently tuned over the range 200–500 nm and 5–20 nm respectively.

The resulting hierarchical pore network of a propylsulfonic acid functionalised macro-mesoporous SBA-15, illustrates how macropore incorporation confers a striking enhancement in the rates of tricaprylin transesterification and palmitic acid esterification with methanol, attributed to the macropores acting as transport conduits for reactants to rapidly access $PrSO_3H$ active sites located within the mesopores.

ZnO is a heterogeneous photocatalyst which has been used for the degradation of organic pollutants in water and air under UV irradiation[164–167] and for the photoepoxidation of propene by molecular oxygen.[168] ZnO/SiO_2 has also been trialled in biodiesel production from crude Mexican *Jatropha curcas* oil *via* a two-step process[169] in which fatty acids were photocatalytically esterified with MeOH under high energy UVC light unrepresentative of the solar spectrum at ground level. Thermally activated transesterification was subsequently performed employing homogeneous NaOH. Porosimetry and IR studies showed no room temperature CO_2 or H_2O adsorption suggesting this catalyst should be stable for low temperature esterification. ZnO/SiO_2 gave >95% FFA conversion after 8 h of UV irradiation (Fig. 8), with activity constant even after 10 successive runs, although loss of solid catalyst between recycles resulted in a final conversion of only ~20% per run, albeit using very high catalyst loadings. Reaction was proposed to occur *via* FFA adsorption at Lewis acidic Zn^{2+} and MeOH at lattice oxygen, followed by photon adsorption by ZnO and the reaction of photogenerated holes to form H^+ and $CH_3O^\bullet$ radicals, with photogenerated electrons reacting with adsorbed

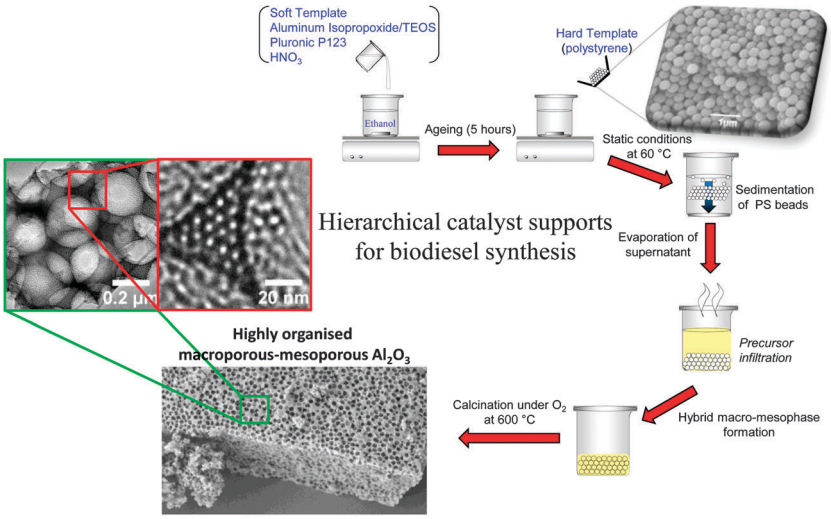

Scheme 4 Liquid crystal and polystyrene nanosphere dual surfactant/physical templating route to hierarchical macroporous–mesoporous silicas.

Open Access Article. Published on 24 June 2014. Downloaded on 1/3/2025 11:41:55 PM.
This article is licensed under a Creative Commons Attribution 3.0 Unported Licence.

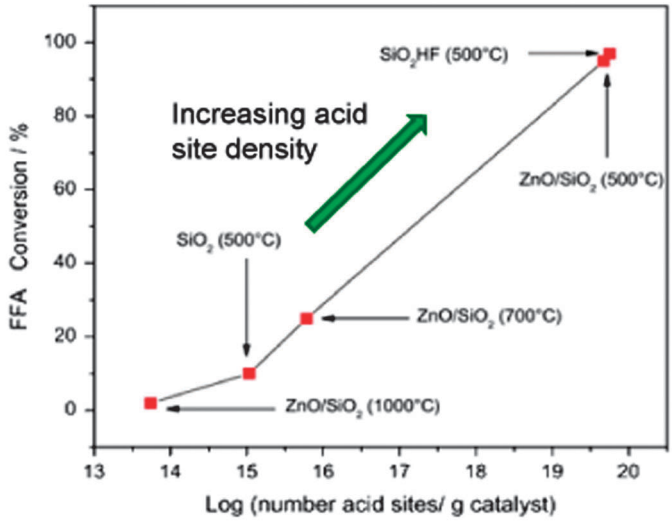

Catalyst	Calcination temperature (°C)	Specific surface area (m^2 g cat^{-1})	Acid sites·g cat^{-1}	FFA conversion (%)
SiO_2	500	200	1.07×10^{15}	10
SiO_2·HF	500	140	5.75×10^{19}	97
1% ZnO/SiO_2	500	185	4.68×10^{19}	95
1% ZnO/SiO_2	700	86	6.02×10^{15}	25
1% ZnO/SiO_2	1000	66	5.5×10^{13}	2

More acid sites = superior catalytic activity

Fig. 8 Relationship between acid site density and catalytic performance in FFA esterification. Adapted from ref. 171. Copyright (2014), with permission from Elsevier.

acids to form •HOOCR radicals; protons and free radicals then reacted to generate intermediates and products. No spectroscopic or chromatographic evidence was presented in support of this elaborate mechanism. Despite the advantages afforded by the ZnO/SiO_2 photocatalyst for low temperature FFA esterification, the use of a conventional soluble base in the transesterification step and consequent washing and saponification issues remains problematic, and scale-up of such photocatalysed batch processes to deliver a significant volume of biodiesel will require new photoreactor designs. ZnO/SiO_2 materials are also active for the thermally-driven esterification of FFAs (although no details were provided on the nature of these fatty acids) within *Jatropha curcas* crude oils, wherein activity was proportional to acid site density.[170]

In summary, recent developments in tailoring the structure and surface functionality of mesoporous silicas has led to a new generation of tunable solid acid catalysts well-suited to the esterification of short and long chain FFAs, and transesterification of diverse TAGs, with methanol under mild reaction conditions. A remaining challenge is to extend the dimensions and types of pore-interconnectivities present within the host silica frameworks, and to find alternative low cost soft and hard templates to facilitate synthetic scale-up of these catalysts for multi-kg production. Surfactant template extraction is typically achieved *via* energy-intensive solvent reflux, which results in significant volumes of contaminated waste and long processing times, while colloidal templates often require high temperature calcination which prevents template recovery/re-use and releases carbon dioxide. Preliminary steps towards the former have been recently taken, employing room temperature ultrasonication in a small solvent volume to deliver effective extraction of the P123 Pluronic surfactant used in the preparation of SBA-15 in only 5 min, with a 99.9% energy saving and 90% solvent reduction over reflux methods, and without compromising textural, acidic or catalytic properties of the resultant Pr-SO_3H-SBA-15 in hexanoic acid esterification (Fig. 9).[171]

4.2 Heteropolyacids

Heteropolyacids are another interesting class of well-defined acid catalysts, capable of exhibiting superacidity ($pK_{H^+} > 12$) and possessing flexible structures.[172] In their native form, heteropolyacids are unsuitable as heterogeneous catalysts for biodiesel applications due to their high solubility in polar media.[173] Dispersing such polyoxometalate clusters over traditional high area oxide supports can modulate their acid site densities,[174,175] but does little to improve their solubility during alcoholysis. Ion-exchanging larger cations into Keggin type phospho- and silicotungstic acids can increase their chemical stability. For example, Cs salts of phosphotungstic acid $Cs_xH_{(3-x)}PW_{12}O_{40}$ and $Cs_yH_{(4-y)}SiW_{12}O_{40}$ are virtually insoluble in water, with proton substitution accompanied by a dramatic increase in surface area of the resulting crystallites.[137,176] As a consequence of these enhanced structural properties, albeit at the expense of losing acidic protons, both $Cs_xH_{(3-x)}PW_{12}O_{40}$ and $Cs_yH_{(y-x)}SiW_{12}O_{40}$ are active for palmitic acid esterification to methyl palmitate and tributyrin transesterification (Fig. 10).

Open Access Article. Published on 24 June 2014. Downloaded on 1/3/2025 11:41:55 PM.
This article is licensed under a Creative Commons Attribution 3.0 Unported Licence.

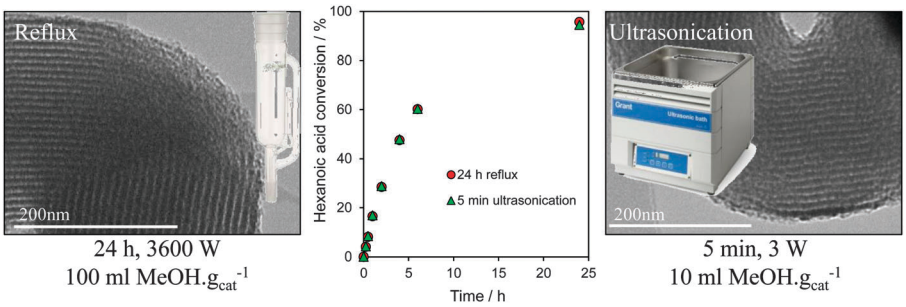

Fig. 9 Surfactant template extraction *via* energy/atom efficient ultrasonication delivers a one-pot $PrSO_3H$-SBA-15 solid acid catalyst with identical structure and reactivity to that obtained by conventional, inefficient reflux. Adapted from ref. 172 with permission from The Royal Society of Chemistry.

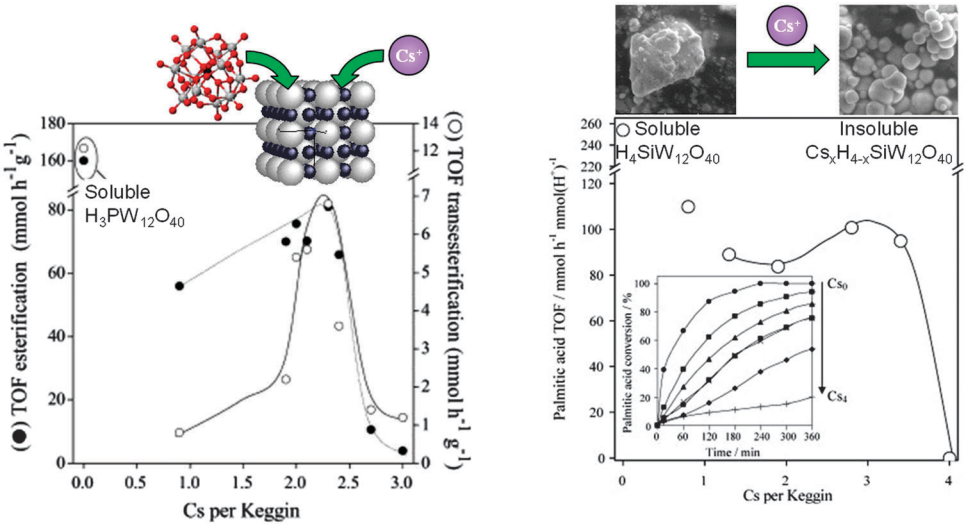

Fig. 10 Impact of Cs ion-exchange into (left) both $Cs_xH_{(3-x)}PW_{12}O_{40}$ for palmitic acid esterification and tributyrin transesterification with methanol; and (right) and $Cs_yH_{(y-x)}SiW_{12}O_{40}$ for palmitic acid esterification, benchmarked against parent fully protonated, soluble clusters. Adapted from ref. 138 and 177. Copyright (2007 and 2009), with permission from Elsevier.

For $Cs_xH_{(3-x)}PW_{12}O_{40}$, optimum esterification and transesterification activity was obtained for x = 2.1–2.4, a similar degree of Cs doping to that maximising palmitic acid esterification for $Cs_yH_{(4-y)}SiW_{12}O_{40}$ catalysts (y = 2.8–3.4). These optimal compositions reflect a maximum in the density of accessible surface acid sites within the insoluble Cs-doped catalysts. For $Cs_yH_{(4-y)}SiW_{12}O_{40}$, wherein C_4 and C_8 TAG transesterification were compared, the absolute reaction rates were faster for the shorter chain triglyceride, attributed to slow in-pore diffusion of the longer chain oil. Absolute TOFs for tributyrin transesterification over the optimised Cs-doped catalyst were greater than for the homogeneous $H_4SiW_{12}O_{40}$ polyoxometalate clusters, a consequence of the greater hydrophobicity of the $Cs_xSiW_{12}O_{40}$ salts compared with the parent $H_4SiW_{12}O_{40}$, which thus afford enhanced activity for the more lipophilic C_8 TAG. Optimising the heterogeneous catalytic activity of $Cs_yH_{4-y}SiW_{12}O_{40}$ requires a balance between the retention of acidic protons and generation of stable mesopores to facilitate molecular diffusion. Cs ion-exchange generates interparticle voids large enough to accommodate short-chain TAGs and longer saturated FFAs. Oil/fatty acid and biodiesel polarity and associated mass transport to/from active acid sites is obviously critical in regulating reactivity, and an area where improved materials design in conjunction with molecular dynamics simulations will offer further avenues for high-performance heteropolyacid catalysts.

Duan *et al.* have prepared $H_3PW_{12}O_{40}$ supported on magnetic iron oxide particles (MNP-HPA) *via* an acid–base interaction and tested them in palmitic acid esterification with methanol under mild conditions.[177] The magnetic nanoparticles were first coated in a protective SiO_2 layer and then functionalised with aminopropyl groups, with the heteropolyacid immobilised by reaction with the amine. Water tolerance was imbued by the addition of nonyl chains to the catalyst surface which lowered the acid loading but improved palmitic acid conversion to 90% at 65 °C. Magnetic separation enabled catalyst recycling without activity loss (Fig. 11), while the presence hydrophobic/oleophilic nonyl groups improved diffusion of the reagent to the active sites, enhancing TOFs compared to the parent MNP-HPA. However, the water tolerance of these materials was limited, with only 1 wt% water reducing FFA conversion to 34%.

Mesostructured silicas have also been employed as supports for HPAs, for example 12-tungstophosphoric acid (TPA) dispersed over mesoporous MCM-48 is a promising solid acid

Open Access Article. Published on 24 June 2014. Downloaded on 1/3/2025 11:41:55 PM.
This article is licensed under a Creative Commons Attribution 3.0 Unported Licence.

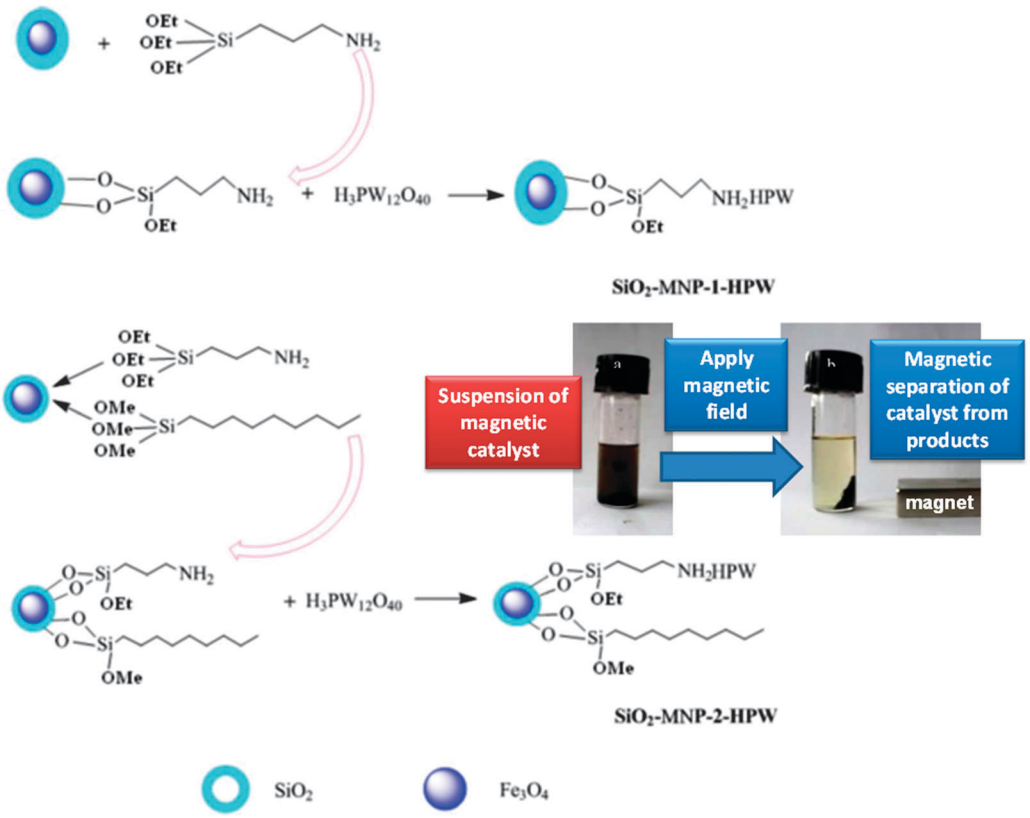

Fig. 11 Preparation of water-tolerant heteropolyacid on magnetic nanoparticles for palmitic acid esterification. Reprinted from ref. 178 with permission from The Royal Society of Chemistry.

catalyst for oleic acid esterification with methanol.[178] This catalyst gave 95% conversion to biodiesel with modest alcohol : acid molar ratios, but very high catalyst loadings (30 wt% TPA). Leaching studies employing insensitive colorimetric tests, suggested good catalyst water stability, with minimal loss of W from MCM-48 detectable by atomic absorption (rather than more sensitive ICP), and retention of the majority of acid sites post-reaction (1.50 mmol g^{-1}). No explanation was advanced for this extremely surprising water tolerance of TPA, which usually exhibits a high solubility in methanol; entrapment of primary Keggin units within the 3 nm diameter MCM-48 pores seems improbable, and any physical barrier to their dissolution would also likely hinder FFA and FAME access to TPA acid sites. The principal disadvantage of heteropolyacids for esterification and transesterification reactions in short-chain alcohols thus remains their limited water tolerance, which to date can only be overcome through advanced catalyst design and the sacrifice of their high acid strength and site density.

4.3 Acidic polymers and resins

While inorganic frameworks such as SBA-15 or ZrO_2 are popular supports for solid acid catalysis, their hydrophilic nature can hinder diffusion of organic reagents. This problem can be avoided by the use of hydrophobic and oleophilic supports, such as mesoporous organic polymers. Sulfonated mesoporous polydivinylbenzene (PDVB) is one such solid acid catalyst,[179] which exhibits absorption capacities for sunflower oil and methanol three times those of $H_3PO_{40}W_{12}$, sulfonated-ZrO_2, SBA-15-SO_3H or Amberlyst 15, and consequent superior performance in tripalmitin transesterification, giving an 80% yield of methyl palmitate after 12 h reaction. PDVB-SO_3H proved easily recyclable, with only a modest drop in yield after three recycles, ascribed to a combination of its high surface area, large pore volume, high acid site density, and hydrophobic/oleophilic pore network. Liu *et al.* utilised an aminophosphonic acid resin based on a polystyrene backbone in the microwave-assisted esterification of stearic acid with EtOH.[180] FAME yields of 90% were obtained after microwave heating to (notionally) 80 °C for 7 h at a catalyst loading of 9 wt%, with slower reaction and a lower limiting conversion of 88% resulting from conventional heating. Kinetic analysis suggested a pseudohomogeneous mechanism in which microwave radiation excited the polar reactants in the solution phase in addition to the solid catalyst. This resin was structurally stable as determined by XRD, TGA and SEM, and recyclable with 87% acid conversion after five uses (Fig. 12).

The acid exchange resin, Relite CFS, was tested under batch and continuous modes for the simultaneous esterification and transesterification of oleic acid and soybean oil with methanol,[181] evidencing good activity with 80% FAME obtained after 150 min at 100 °C. Unfortunately this resin was deactivated *via* exchange with metals such as iron present in the feedstream

Open Access Article. Published on 24 June 2014. Downloaded on 1/3/2025 11:41:55 PM.
This article is licensed under a Creative Commons Attribution 3.0 Unported Licence.

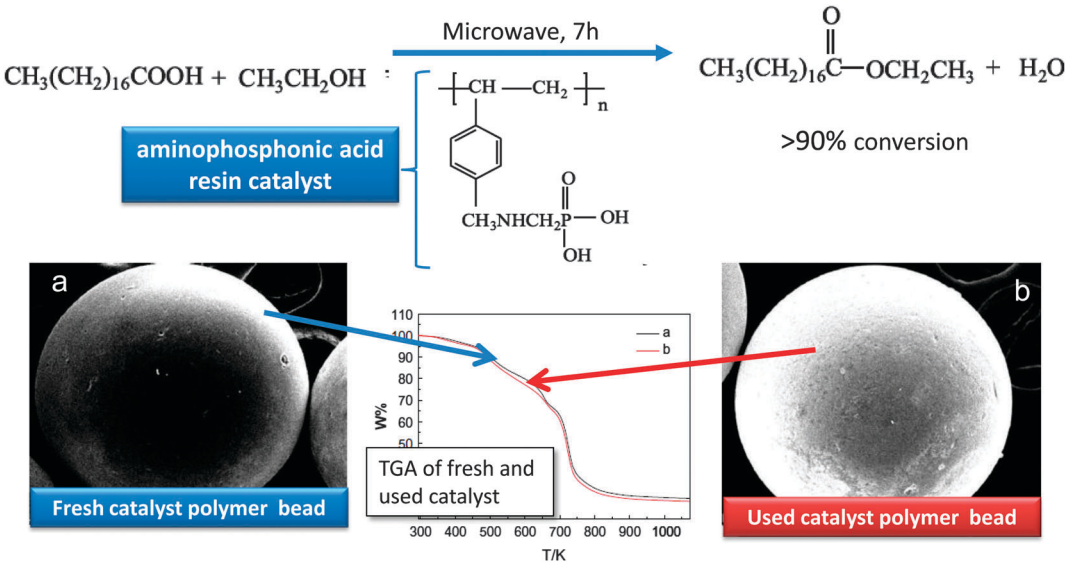

Fig. 12 Stability of a solid acid resin catalyst for stearic acid esterification. Adapted from ref. 181. Copyright (2013), with permission from Elsevier.

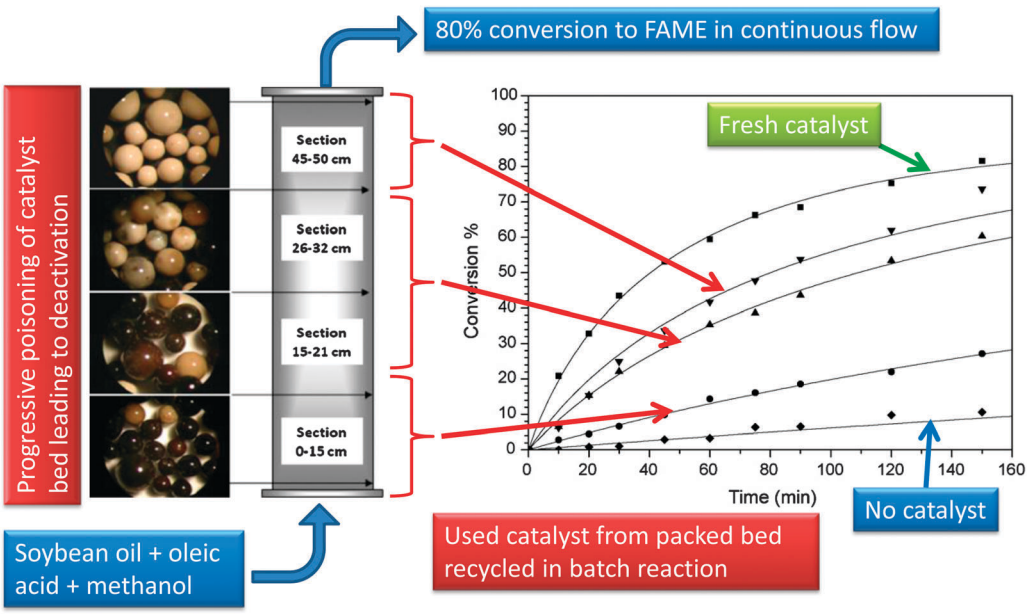

Fig. 13 Deactivation of an acid resin catalyst during continuous esterification/transesterification of FFA and oil mixtures. Adapted from ref. 182. Copyright (2010), with permission from Elsevier.

causing catalyst discolouration of beads during continuous operation (Fig. 13); activity could be completely regenerated by suspending the resin in sulphuric acid for 24 h and a further lengthy washing and drying protocol. A copolymer of acidic ionic liquid oligomers and divinylbenzene (PIL) has also been utilised as a catalyst for simultaneous esterification and transesterification of FFA-containing triglyceride mixtures (waste cooking oil), possessing a high acid density of 4.4 mmol g^{-1}, high pore volume and surface area of 323 m^2 g^{-1}, and 35 nm mean pore diameter.[182] The latter and hydrophobic surface character permitted efficient substrate diffusion through the pore network. The PIL copolymer was more active than the acidic ionic liquid alone, giving >99% conversion of oleic acid with MeOH at only 1 wt% catalyst loading. PIL also achieved >99% yield in rapeseed transesterification with MeOH under the same reaction conditions, and proved able to convert high FFA content waste cooking oil into biodiesel with 99% yield in 12 h. The spent catalyst showed no structural changes or loss of acidic sulphur, and hence could be efficiently recycled with almost no loss in performance.

4.4 Waste carbon-derived solid acids

As discussed earlier in this review, many studies have investigated the development of carbon catalysts prepared from

Open Access Article. Published on 24 June 2014. Downloaded on 1/3/2025 11:41:55 PM.
This article is licensed under a Creative Commons Attribution 3.0 Unported Licence.

second generation biomass such as non-edible crop waste,[2,106,107] algal residues[108] and even waste products from biodiesel production.[109] Sulfonated carbonaceous materials show promising activity for FFA esterification, generally affording higher rates of biodiesel production than commercial resins such Amberlyst with which they are often compared.

Residue of the non-edible seed *Calophyllum inophyllum* has been carbonised to make a biomass-derived solid acid catalyst *via* sulfonation.[107] The resulting catalysts, comprising randomly oriented, amorphous aromatic sheets of low surface area (0.2 to 3.4 m^2 g^{-1}) and variable acid densities (0.6 to 4.2 mmol g^{-1} dependent on the S wt%), were tested in the simultaneous esterification and transesterification of *Calophyllum inophyllum* seed oil. Esterification activity was greatly proportional to the S loading, but also influenced by the balance of hydrophobic/hydrophilic sites on the carbon which affected diffusion and adsorption of oleo substrates. This balance, and related surface properties, varied with the carbonisation and sulphonation conditions employed; short carbonisation times lead to smaller sheets with higher SO_3H densities and increased activity, but also increased S leaching and concomitant deactivation. Rice husk char was sulfonated with concentrated sulfonic acid under various conditions, and evaluated in the esterification of oleic acid with MeOH.[2] All catalysts were amorphous, with a maximum SO_3H density of 0.7 mmol g^{-1}. High conversions were obtained at 110 °C in 2 h for a low alcohol : oil molar ratio of 4 : 1, with the catalyst recyclable and still delivering 84% methyl oleate after seven re-uses despite losing 23% of the initial S through leaching.

Peanut shells processed in a similar manner to that above also yield a strong Brönsted solid acid catalyst, with an acid strength superior to H-ZSM-5 (Si/Al = 75).[183] This catalyst gave >90% conversion of cottonseed oil in methanol transesterification at a methanol : oil molar ratio of only 9 : 1. Recycling and re-use studies employed centrifugation to separate the catalyst, with subsequent acetone washes leading to a 50% reduction in acid site density, although regeneration was achievable by prolonged treatment with 1 M H_2SO_4 solution. Despite the environmental compatibility of waste biomass-derived solid acid catalysts, active site retention over prolonged use remains a critical challenge if they are to find implementation in continuous biodiesel production; leaching of sulphate or sulfonic acid groups into the product stream would both shorten catalyst lifetime and degrade fuel quality.

Microalgae are an exciting, potential feedstock for biodiesel production, but following extraction of algal oils, the residue is typically burned or discarded. Fu *et al.*[108] has partially carbonised and sulfonated such residue to create a solid acid catalyst for the esterification of oleic acid and transesterification of triolein with methanol at 80 °C (Fig. 14). Although the resulting catalyst comprised disordered, non-porous aromatic carbon sheets with a very low surface area, the sulfonic acid density of 4.25 mmol g^{-1} afforded an active catalyst with a stable FFA conversion >98% over six sequential oleic acid esterification cycles. The corresponding FAME yield for triolein transesterification was only 22%, but likewise stable across numerous recycles. However, such catalysts were prone to deactivation by adsorbed methanol and hence required regenerative sulphuric acid and hot water washes between recycles. A similar approach was adopted for the waste glycerol by-product of biodiesel production, whereby the polyol was converted *in situ* by partial carbonisation and sulfonation into a solid acid catalyst.[109] High catalyst loadings, reaction temperatures (160 °C) and MeOH : oil ratios (>45) were required to achieve 99% conversion of Karanja oil to FAME, with conversion dropping to only 5% after five recycles, although no analysis of the spent catalyst or leaching studies were reported. Leaching of acid sites was however addressed by Deshmane *et al.*,[184] who investigated sulfonated carbon catalysts prepared from sugar and polyacrylic acid for oleic acid esterification. These catalysts were deactivated by the formation of irregularly-shaped, 1 μm colloidal carbon aggregates, comprised of sulfonated polycyclic hydrocarbons, during the hydrothermal, sulfonation or pulverisation preparative steps, which subsequently leaching into the esterification reaction mixture.

The kinetics of palm oil fatty acid esterification with MeOH over carbonised, sulfonated microcrystalline cellulose (CSMC) have also been compared with those of homogeneous sulphuric

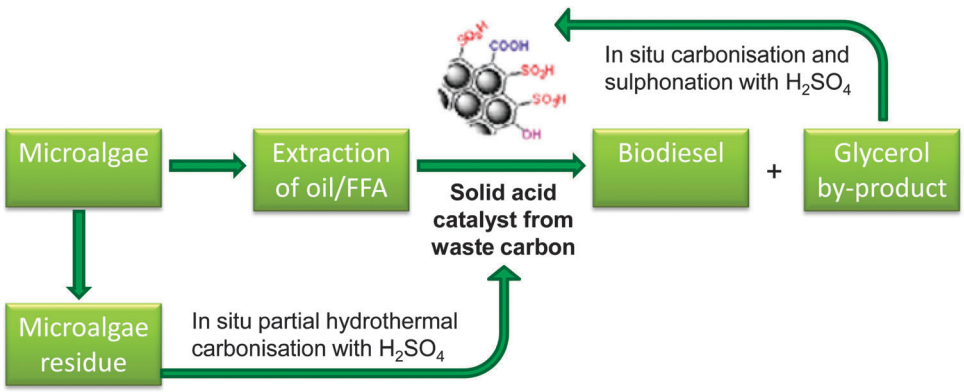

Fig. 14 Microalgae as a source of bio-oils/fatty acids for biodiesel production, and waste, biomass residue for the synthesis of solid acid catalysts to drive such biodiesel production.

Open Access Article. Published on 24 June 2014. Downloaded on 1/3/2025 11:41:55 PM.
This article is licensed under a Creative Commons Attribution 3.0 Unported Licence.

acid catalysts,[185] compensating for the phase equilibrium and reaction equilibrium to provide an accurate kinetic reaction model; this approach ensured the biphasic nature of the water–alcohol–oil reaction mixture was correctly represented instead of assuming a pseudo-homogeneous model. Methanol and FFA adsorption over the CSMC was believed a key step in the heterogeneous process, and hence adsorption equilibrium constants were calculated for these molecules along with water and FAME. Unsurprisingly, the free fatty acid was found to adsorb preferentially in the presence of low concentrations of the other molecules. At the start of the esterification reaction, FFA and alcohol were fully miscible, but water and FAME production led to the evolution of two phases; one comprising aqueous methanol and catalyst, and the other methyl ester and unreacted FFA. Mass-transport between these phases is essential, but likely the rate-limiting step. Kinetics of both homogeneously and heterogeneously catalysed biphasic systems were modelled with high conversions favoured by the limited solubility of water in the organic phase, and the use of hydrophobic catalysts which displace water from reaction sites.

A major drawback of the preceding sulfonated carbons is their low surface area, which can be alleviated through the use of carbon nanotubes. Poonjarernsilp and co-workers prepared solid acid catalysts by sulfonating single-walled carbon nanohorns (SWCNHs)[186] which possessed surface areas of 210 $m^2\ g^{-1}$ and could be further improved by high temperature calcination to open up micropores. The resulting oxidised nanohorns (ox-SWCNs) had surface areas of 1000 $m^2\ g^{-1}$ and superior pore volumes. However the subsequent sulfonation step required to introduce surface acidity, somewhat lowered the final surface area and pore volume, and drastically altered the pore size distribution, eliminating all the meso- and macropores to leave a narrow range of 2–10 nm pores. Despite the improved morphology of the sulfonated ox-SWCNs relative to the SWCNs, the former had a lower acid site density and was consequently less active in palmitic acid the esterification with methanol; the best yield was obtained for SO_3H-SWCNHs, which gave 93% methyl palmitate after 5 h with a catalyst : MeOH : FFA ratio of 0.15 : 0.15 : 5 g. Recycling tests showed a progressive decrease in methyl palmitate yield associated with a loss of acid sites.

4.5 Miscellaneous solid acids

A range of additional solid acids have also been investigated, including ferric hydrogen sulphate $[Fe(HSO_4)_3]$,[187] supported tungsten oxides (WO_3/SnO_2),[188] supported partially substituted heteropolytungstates,[189] and bifunctional catalysts, such as Mo-Mn/Al_2O_3-15 wt% MgO,[190] designed to incorporate the benefits of both acid and base catalysis. The iron catalyst had a low surface area of 4–5 $m^2\ g^{-1}$, and required higher operating temperatures than other solid acids to achieve good biodiesel yields (94% at 205 °C),[187] but was easily recycled by simple washing and drying to remove adsorbed products, maintaining activity over 5 cycles with no evidence of metal leaching. WO_3/SnO_2 was water tolerant and showed good conversion of soybean oil to FAME at a lower reaction temperature (110 °C), but required high MeOH : oil ratios >30 to achieve a 78% yield,[188] but was prone to on-stream deactivation upon recycling. Tungsten-containing HPAs supported on silica, alumina, and zirconia were also active in biodiesel production from 10 wt% oleic acid in soybean oil delivering FAME yields >75% at a high reaction temperature. Performance was unaffected by the presence of up to 25 wt% of the fatty acid blended with the oil. Cesium addition to the HPA suppressed leaching and thereby improved catalyst stability, resulting in only a 10% fall in biodiesel production after multiple recycles attributed to physical sample loss during product separation.

In an attempt to incorporate acid and base character in a single material, Farooq *et al.* prepared a Mo-Mn/γ-Al_2O_3-15 wt% MgO catalysts *via* wet impregnation of alumina with MgO, followed by impregnation of the γ-Al_2O_3-MgO with $[(NH_4)_6Mo_7O_{24}]\cdot 4H_2O$ and subsequently aqueous $Mn(NO_3)_2$.[190] The resulting thermally processed catalyst possessed highly dispersed MoO_3 and MnO acid sites, affording 75% biodiesel yield at 95 °C with a MeOH : oil molar ratio of 15. This bifunctional material could be repeatedly recycled with the yield falling by 20% after 10 uses, a modest deactivation that was attributed to poisoning by strongly adsorbed organics and leaching of the various active metals during transesterification.

5. Hydrophobicity studies

The hydrophilic nature of polar silica surfaces hinders their application for reactions involving apolar organic molecules. This is problematic for TAG transesterification (or FFA esterification) due to preferential in-pore diffusion and adsorption of alcohol *versus* fatty acid components. The presence of water in bio-oils (and an inevitable by-product of esterification) can significantly influence biodiesel production, however a major barrier to commercialisation is the development of an efficient, inexpensive and reusable heterogeneous catalyst that can perform at low temperature and pressure.[191] Solid catalysts with ordered and large pores to minimise diffusion limitations, moderate to strong acid sites to overcome the presence of FFAs impurities, and a hydrophobic surface to nullify the effect of water are hence sought.[32,192–196] While solid acid catalysts are of great interest in this regard due to their ability to catalyse both FFA esterification and TAG transesterification,[144,197] sensitivity to water is a common cause of deactivation,[198,199] and water-tolerant solid acids would be highly desirable.[31,37,200] Surface hydrophobicity, and the relative adsorption/desorption rates of reactants/products, are critical parameters influencing (trans)esterification,[201] and tuning catalyst polarity thus offers a route to control competitive adsorption and promote product desorption. Steric factors associated with long fatty acid alkyl chains can also influence reaction rates;[202] Alonso and co-workers explored the relationship between fatty acid polarity/chain length (C_2–C_{16}) and transesterification rates over solid and liquid acid catalysts.[203] Activity decreased with increasing chain length for a heterogeneous (SAC-13) catalyst, but remained constant when catalysed by H_2SO_4, highlighting the negative impact of hydrophilic surfaces on biodiesel production.[203]

Surface hydroxyl groups favour H_2O adsorption, which if formed during FFA esterification can drive the reverse hydrolysis reaction and lowering FAME yields. Surface modification *via* the incorporation of organic functionality into polar oxide

Open Access Article. Published on 24 June 2014. Downloaded on 1/3/2025 11:41:55 PM.
This article is licensed under a Creative Commons Attribution 3.0 Unported Licence.

surfaces, or dehydroxylation, can lower their polarity and thereby increase initial rates of acid catalysed transformations of liquid phase organic molecules.[204] Surface polarity can also be tuned by incorporating alkyl/aromatic groups directly into the silica framework, for example polysilsesquioxanes can be prepared *via* the co-condensation of 1,4-bis(triethoxysilyl)benzene (BTSB), or 1,2-bis(trimethoxysilyl)-ethane (BTME), with TEOS and MPTS in the sol–gel process[205,206] which enhances small molecule esterification[207] and etherification.[208] This approach has been adopted for the direct synthesis of Lewis acidic, zirconium-containing periodic mesoporous organosilicas (Zr-PMOs), in which zirconocene dichloride was employed as the zirconium source and BTEB was progressively substituted for TEOS.[209] The resulting organosilanes were topologically similar to a purely inorganic Zr-SBA-15 material, but are strongly hydrophobic in nature. Although the one-pot metal doping protocol adopted resulted in relatively low densities of Zr incorporated into the final solid catalyst, hydrophobisation significantly enhanced the per acid site activity in the simultaneous esterification of FFAs and transesterification of TAGs in crude palm oil with methanol at 200 °C, with conversions approaching 90% after only 6 h (Fig. 15). As significant, the catalytic performance of the high organic content Zr-PMO materials was barely influenced by the addition of up to 20 wt% water to the feedstock, in contrast to the inorganic Zr-SBA-15 analogue which was completely poisoned by such water addition. The high water and fatty acid tolerance of these Zr-PMO catalysts renders them especially promising for biodiesel production from waste oil sources.

The incorporation of organic spectator groups (*e.g.* phenyl, methyl or propyl) during the sol–gel syntheses of SBA-15[210] and MCM-41[211] sulphonic acid silicas is also achievable *via* co-grafting or simple addition of the respective alkyl or aryltrimethoxysilane during co-condensation protocols. An experimental and computational study of sulphonic acid functionalised MCM-41 materials was undertaken in order to evaluate the effect of acid site density and surface hydrophobicity on catalyst acidity and associated performance.[212] MCM-41 was an excellent candidate due to the availability of accurate models for the pore structure from kinetic Monte Carlo simulations,[213] and was modified with surface groups to enable dynamic simulation of sulphonic acid and octyl groups co-attached within the MCM-41 pores. In parallel experiments, two catalyst series were investigated towards acetic acid esterification with butanol (Scheme 5). In one series, the propylsulphonic acid coverage was varied between $\theta(RSO_3H)$ = 0–100% ML over the bare silica (MCM-SO_3H). For the second octyl co-grafted series, both sulfonic acid and octyl coverages were tuned (MCM-Oc-SO_3H). These materials allow the effect of lateral interactions between acid head groups and the role of hydrophobic octyl modifiers upon acid strength and activity to be separately probed.

To avoid diffusion limitations, butanol esterification with acetic acid was selected as a model reaction (Fig. 16). Ammonia calorimetry revealed that the acid strength of polar MCM-SO_3H materials increases from 87 to 118 kJ mol^{-1} with sulphonic acid loading. Co-grafted octyl groups dramatically enhance the acid strength of MCM-Oc-SO_3H for submonolayer SO_3H coverages, with $\Delta H_{ads}(NH_3)$ rising to 103 kJ mol^{-1}. The per site activity of the MCM-SO_3H series in butanol esterification with acetic acid mirrors their acidity, increasing with SO_3H content. Octyl surface functionalisation promotes esterification for all MCM-Oc-SO_3H catalysts, doubling the turnover frequency of the lowest loading SO_3H material. Molecular dynamic simulations indicate that the interaction of isolated sulphonic acid moieties with surface silanol groups is the primary cause of the lower acidity and activity of submonolayer samples within the MCM-SO_3H series. Lateral interactions with octyl groups help to re-orient sulphonic acid headgroups into the pore interior, thereby enhancing acid strength and associated esterification activity.

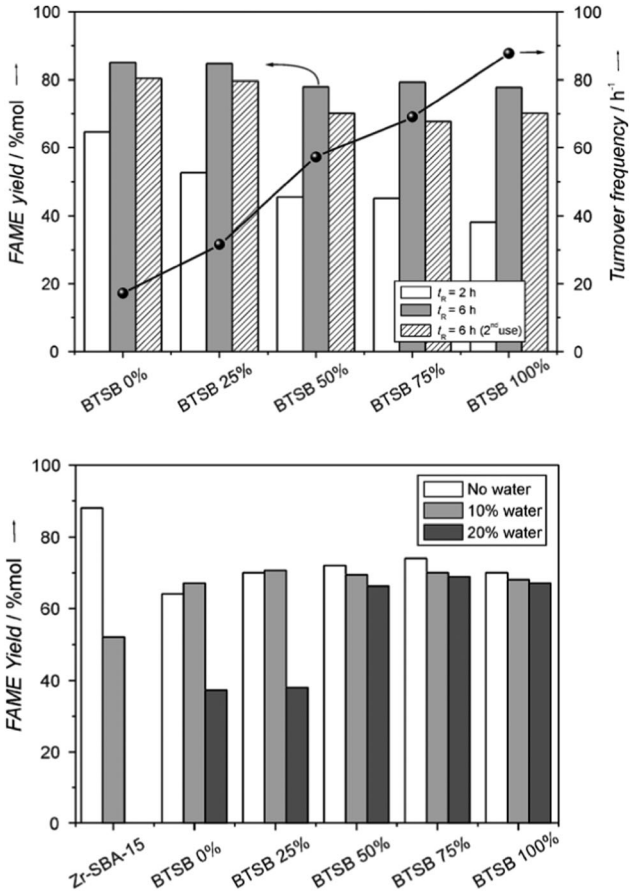

Fig. 15 (top) FAME yield and turnover frequency calculated for Zr-PMO materials in the methanolysis of crude palm oil highlighting the impact of catalyst hydrophobicity; and (bottom) FAME yield as a function of organic content for Zr-PMO materials in the presence of additional water in the crude palm oil reaction media evidencing superior water tolerance of hybrid solid acid catalysts. Reprinted from ref. 210. Copyright 2013 John Wiley and Sons.

In some cases, the introduction of hydrophobic functionalities may actually cap the active catalytic site. For example, post-modification of an arene-sulfonic acid SBA-15 by methoxytrimethylsilane deactivated the catalyst by capping the active sites with methyl groups and changing the textural properties, whereas methyl groups introduced *via* a one-pot synthesis did not affect activity towards the microwave-assisted transesterification of soybean oil with 1-butanol.[214] Ethyl groups may also be

Open Access Article. Published on 24 June 2014. Downloaded on 1/3/2025 11:41:55 PM.
This article is licensed under a Creative Commons Attribution 3.0 Unported Licence.

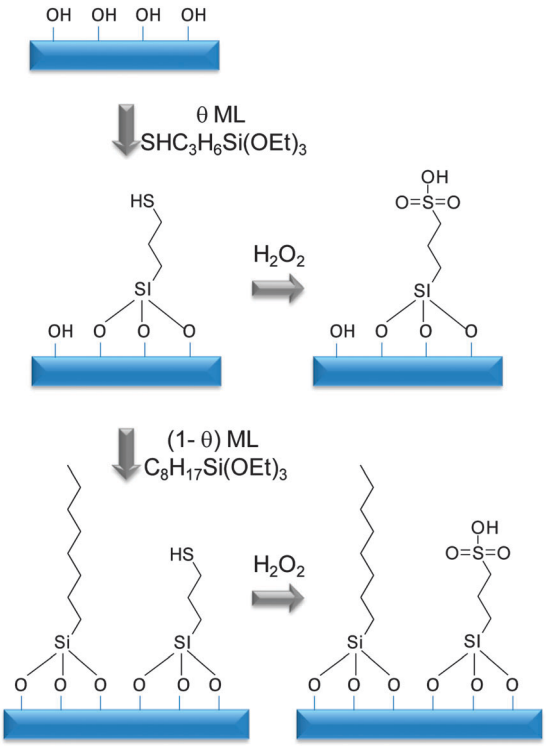

Scheme 5 Protocol for the synthesis of sulfonic acid and octyl co-functionalised sulfonic acid MCM-41 catalysts. Adapted from ref. 213 with permission from The Royal Society of Chemistry.

introduced onto the surface of sulfonic acid modified SBA-15 to impart hydrophobicity. While such ethyl groups has no impact on overall conversions, they improved the initial rate of octanoic acid esterification by displacing reactively-formed water during the start of reaction.[215]

As discussed earlier in this review, hydrophobic solid acid catalysts with large pores are desirable to enhance in-pore mass transport of bulky bio-oils and fatty acids, and to minimise the impact of reactively-formed water during FFA esterification.[37,216] Although many solid catalysts exist with potential in biodiesel production,[154,217] research is increasingly focused on modifying surface hydrophobicity to achieve these goals. Hydrophobicity can be imparted to zeolites by incorporating organic species within their micropores; however, for transesterification involving long chain TAGs, large pore zeolites are preferable, with activity increasing with Si : Al ratio and surface hydrophobicity.[195,218] Fe–Zn double metal cyanides (DMC), possessing only Lewis acid sites, were reported active for sunflower oil transesterification with methanol at 98% conversion. These catalysts exhibited good water tolerance, even in the presence of 20 wt% water in oil, possibly reflecting their surface hydrophobicity and higher coverage of adsorbed reactants.[194] The hydrophobic nature of these catalysts was demonstrated by them in oil–water, water–toluene and water–CCl_4 mixtures, wherein the catalyst remained suspended in the hydrophobic layer (Fig. 17).[201,219] Fe–Zn DMC was

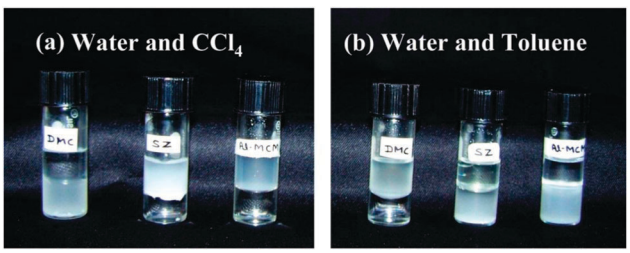

Fig. 17 Preferential dispersion of DMC in the nonpolar, organic phase, and SZ and Al-MCM-41 in the polar aqueous phase of (a) water–CCl_4 and (b) water–toluene solvent mixtures. Reprinted with permission from ref. 202. Copyright 2010 American Chemical Society.

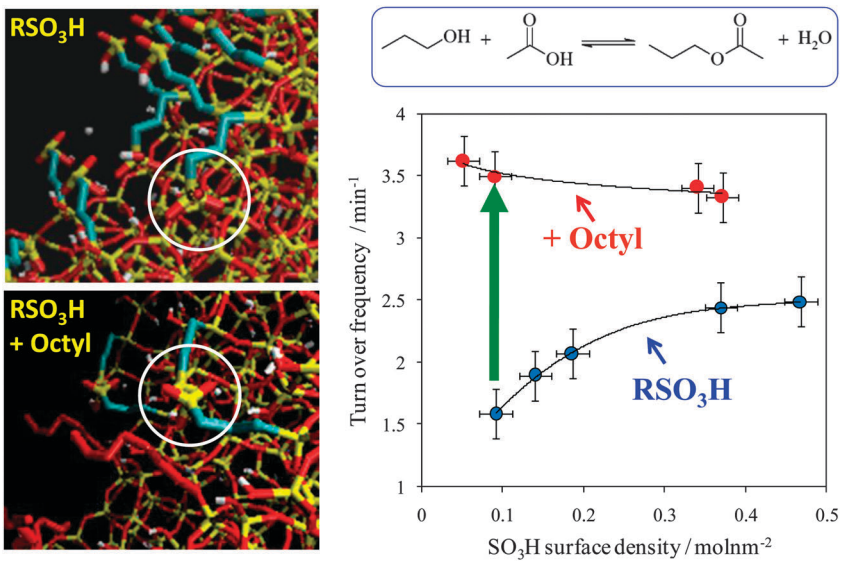

Fig. 16 (left) Molecular dynamics simulations of MCM-SO_3H and MCM-Oc-SO_3H pore models highlighting the interaction between surface sulfonic acid and hydroxyl groups in the absence of co-grafted octyl chains; (right) influence of $PrSO_3H$ surface density and co-grafted octyl groups on catalytic performance in acetic acid esterification with butanol. Adapted from ref. 213 with permission from The Royal Society of Chemistry.

Open Access Article. Published on 24 June 2014. Downloaded on 1/3/2025 11:41:55 PM.
This article is licensed under a Creative Commons Attribution 3.0 Unported Licence.

compared against SZ and Al-MCM-41 for the esterification of long chain (C_8–C_{18}) FFAs, and the transesterification of soybean oil. SZ and Al-MCM-41 showed better conversion than DMC towards the fatty acids, but reverse was observed for the more hydrophobic soybean oil.[201] Fe–Zn DMC possessed a hybrid structure containing both crystalline and amorphous phases; hydrophobicity ascribed to the presence of the latter phase.[220]

Cesium-doped dodecatungstophosphoric acid (CsPW) has shown promise as a water-tolerant solid acid catalyst for the hydrolysis of ethyl acetate,[221] and found subsequent employ in the transesterification of Eruca sativa Gars (ESG) oil.[202] The authors claimed that CsPW exhibited excellent water-tolerance towards ESG transesterification, despite oil conversions falling by ~90% upon the addition of only 1% water. Zn containing HPAs display more impressive credentials for transforming challenging feedstocks, with zinc dodecatungstophosphate nanotubes possessing Lewis and Brönsted acid sites effective for the for the simultaneous esterification and transesterification of palmitic acid, and transesterification of waste cooking oils with 26% FFA and 1% water.

The one-pot synthesis of a styrene modified sulfonic acid silica 15 was achieved by adding styrylethyl-trimethoxysilane during a conventional SBA-15 synthesis.[222] Styryl groups polymerised on the silica surface imparted hydrophobicity. Subsequent acid functionalisation of these materials resulted in a polystyrene-modified sulfonic acid SBA-15, which was active for oleic acid esterification with *n*-butanol, and proved superior to SAC-13 and Amberlyst-15 due to the hydrophobic polystyrene coating and high surface area.[223]

Surface acidity has also been imparted to hydrophobic, mesoporous polydivinylbenzene (PDVB) by sulfonic acid grafting. Such materials were employed in tripalmitin transesterification with methanol, revealing that mesoporous PDVB with electron withdrawing $-SO_3H$–SO_2CF_3 groups gave good activity with 91% yield maintained up to 5 re-uses. Contact angle measurements confirmed the hydrophobic nature and high oleophilicity of these materials. PDVB grafted with chlorosulfonic acid also generated hydrophobic solid acid catalysts for tripalmitin which were successfully transesterification whose performance (80% methyl palmitate yield) was superior to HPA, SBA-15-SO_3H, Amberlyst 15, and mesoporous SO_4–ZrO_2. The same activity trend was observed for sunflower oil transesterification wherein all C_{16}–C_{27} fatty acids were converted to FAMEs reflecting the higher adsorption capacity and hence reactivity of these PDVB acids.[179,223,224] Polyaniline functionalised with methanosulfonic (MSA-Pani), camphorosulfonic (CSA-Pani) and lignosulfonic (LG-Pani) acids and polyaniline sulfate (S-Pani) also show promise in biodiesel synthesis with the LG-Pani catalyst possessing the greatest acid site density (3.62 $mmol_{H^+}\ g^{-1}$) and highest conversion due to the close proximity of hydrophobic centres to the active sites. Sulfonic acid containing ionic liquids have also been co-polymerised with divinyl benzene, to form a hydrophobic, solid acidic ionic liquid polymer (PIL) for the transesterification of rapeseed and waste cooking oils, outperforming homogeneous counterparts.[182]

Partial carbonisation and sulfonation of organic matter offers a route to combine acidity and hydrophobicity into carbon based mesoporous materials.[225,226] Such solids are typically partially amorphous, but offer efficient transesterification of non-edible seed oils.[107] It has proven difficult to introduce organic groups into the surface of ordered mesoporous carbons (OMCs) prepared through high temperature carbonisation, however surface pretreatment with H_2O_2 to introduce hydroxyl anchors enables their subsequent sulfonation and a resulting hydrophobic and stable acid catalyst for oleic acid esterification.[227] Sulfonated single-walled carbon nanotubes (SO_3H-SWCH) have also been investigated for palmitic acid esterification, exhibiting higher activity than other sulfonated carbons, such as oxidized SWCNHs (ox-SWCNHs), activated carbon (AC), and carbon black (CB), attributed to the stronger acidity of SO_3H-SWCH and hydrophobicity of the carbon surface in the vicinity of acid sites,[186] enabling it to even outperform liquid H_2SO_4. Another interesting class of porous hydrophobic catalysts are mesoporous titanosilicates which are active for biodiesel and biolubricant synthesis. Ti incorporation into the surface of mesoporous SBA-12 and SBA-16 generates Lewis acid sites which are active for esterification and transesterification. The high activity of these Lewis acid sites is comparable to that observed for Fe–Zn double metal cyanides.[194] Solid state ^{29}Si NMR studies show that Ti-SBA-16 is more hydrophobic than Ti-SBA-12. In biolubricant synthesis, for which surface hydrophobicity is crucial, Ti-SBA-16 is significantly more active than Ti-SBA-12.[228]

Lipase has also been immobilised on hydrophobic supports with a view to transesterifying water containing oils,[229] wherein small amounts of water improved lipase activity.[230] The application of lipase enzymes can be made more cost-effective by heterogenisation over a solid support, with hydrophobic supports both assisting lipase surface attachment and promoting FFA esterification and bio-oil transesterification. *Burkholderia* lipase supported on hydrophobic magnetic particles for olive oil transesterification gave 70% conversion to FAME even in the presence of up to 10% water and was readily recycled.[231] FAME production from canola oil was also achieved using lipase immobilised on a hydrophobic, microporous styrene-divinylbenzene copolymer, wherein the support hydrophobicity mitigated the inhibitory effect of water and glycerol affording a 97% yield.[232]

Solid basic hydrotalcites also showed enhanced activity and reusability for soybean oil transesterification when dispersed over polyvinylalcohol (PVA) membranes, although increasing the hydrophobicity *via* polymer cross-linking lowered activity, presumably due to poor active site accessibility by the bulky substrate. Hydrophilicity *versus* hydrophobicity may be tuned over such membranes by succinic anhydride and acetic anhydride treatments, with a mix of hydrophilic and hydrophobic environments near the active hydrotalcite sites required for optimal transesterification.[233]An interesting contrast to the preceding systems (wherein water poisons FAME formation) was reported for CaO catalysed soybean transesterification, for which small amounts of water actually improve activity, attributed to an increase in the concentration of surface OH- active base sites.[234] Mixed MgO–CaO also exhibited a surprising water tolerance in rapeseed oil transesterification, enabling 98%

Open Access Article. Published on 24 June 2014. Downloaded on 1/3/2025 11:41:55 PM.
This article is licensed under a Creative Commons Attribution 3.0 Unported Licence.

conversion with 2% water, with La_2O_3–CaO active even in the presence of 10% water.[235,236]

Periodic Mesoporous Organosilicas (PMOs) are a promising class of materials that can be used as catalyst supports for biodiesel production. PMOs are hybrid organic–inorganic materials with mesopore networks akin to SBA-15.[236] Functionalisation of PMOs with catalytically active organic moieties is an emergent field of heterogeneous catalysis, and since the organic groups are dispersed throughout the framework (rather than confined to hydroxylated patches of the surface[212]), active sites and hydrophobic centres can be co-located in high concentrations. Methylpropyl sulfonic acid functionalised phenylene- and ethyl-bridged PMOs have been synthesised and tested for the transesterification of sunflower oil, canola oil, corn oil, refined olive oil and olive sludge.[237] These functionalised PMOs gave comparable or better activity than SBA-15-$PrSO_3H$ under optimised conditions, with the ethyl-bridged PMO showing highest activity with a 98% yield. Water adsorption studies proved that the phenylene-bridged PMO was more hydrophobic than the ethyl-bridged variant, but less active, showing that a balance of hydrophobic *versus* hydrophilic mesostructural properties are necessary for optimum transesterification.

Heterogeneous catalysts with tunable hydrophobicity, acid/base character, and good thermal stability, whether based upon polymeric or inorganic frameworks, are hence promising new solutions to TAG transesterification and FFA esterification of high moisture content feedstocks.

6. Influence of reactor design and operating conditions

One other development likely to impact on the commercial exploitation of heterogeneous catalysts for biodiesel production is the design of innovative chemical reactors to facilitate continuous processing of viscous bio-oils. Although many industrial biodiesel production plants operate in batch mode at a significant scale ($\sim$7000 tons year^{-1}),[238–240] there is a need to move towards heterogeneously catalysed, continuous flow reactors in order to avoid the separation issues of homogeneous catalysts and drawbacks of batch mode (notably increased capital investment required to run at large volumes and increased labour costs of a start/stop process)[241] and increase the scale of operation (8000–125 000 tons year^{-1}).[239,240] A range of process engineering solutions have been considered for the continuous esterification of FFAs, including the use of fixed bed[242] or microchannel-flow reactors,[243] pervaporation methods,[244] and reactive distillation.[245,246] Process intensification methods in biodiesel production have been reviewed in depth elsewhere.[247,248]

Reactive distillation combines chemical conversion and separation steps in a single stage. This simplifies the process flow sheets, reduces production costs, and extends catalyst lifetimes through the continuous removal of water from the system. However, this technique is only applicable if the reaction is compatible with the temperatures and pressures required for the distillation. Kiss *et al.* demonstrated this approach for the esterification of dodecanoic acid with a range of alcohols catalysed by sulphated zirconia.[245] Their reactive distillation was 100% selective, permitted shorter residence times than comparable flow systems, and did not require excess alcohol. The latter is a major advantage over the overwhelming majority of conventional biodiesel syntheses wherein, since reaction between the triglyceride and alcohol is reversible, large alcohol excesses are normally required to achieve full conversion (the excess alcohol must then be separated and re-used to ensure economic process viability).

Any continuous flow reactor must be designed appropriately to harness the full potential of the integrated heterogeneous catalyst; plug flow is a desirable characteristic since it permits tight control over the product composition, and hence minimises downstream separation processes, and associated capital investment and running costs. Conventional plug flow reactors are ill-suited to slow reactions such as FFA esterification and TAG transesterification, since they require very high length : diameter ratios to achieve good mixing, and in any event are problematic due to their large footprints and pumping duties, and control difficulties. Oscillatory Baffled Reactors (OBRs) circumvent these problems by oscillating the reaction fluid through orifice plate baffles to achieve efficient mixing and plug flow,[249] thereby decoupling mixing from the net fluid flow in a scalable fashion, enabling long reaction times on an industrial scale, and have been applied to homogeneously catalysed biodiesel synthesis.[250] Vortical mixing in the OBR also offers an effective, controllable method of uniformly suspending solid particles and was recently utilised to entrain a $PrSO_3H$-SBA-15 mesoporous silica within a glass OBR under an oscillatory flow for the continuous esterification of propanoic, hexanoic, lauric and palmitic acid (Fig. 18).[42] Excellent semi-quantitative agreement was obtained between the kinetics of hexanoic acid esterification within the OBR and a conventional stirred batch reactor, with fatty acid chain length identified as a key predictor of solid acid activity. Continuous esterification within the OBR improved ester yields compared with batch operation due to water by-product removal from the catalyst reaction zone, evidencing the versatility of the OBR for heterogeneous flow chemistry and potential role as a new clean catalytic technology.

Phase equilibria considerations are very important in biodiesel production *via* TAG transesterification with methanol, since the reactant and alcohol are generally immiscible, whereas the FAME product is miscible, hampering mass transport and retarding reaction. Separation and purification of the product phase, a mixture of solid catalyst, unreacted oil, glycerol and biodiesel, adds further complexity and cost to production.[251] These problems may be alleviated through the use of membrane reactors,[252–256] wherein the reactor walls are made of a semi-permeable material designed to allow passage of the FAME/glycerol phase, while retaining the oil-rich/MeOH emulsion for further reaction. Xu *et al.* utilised a MCM-41 supported *p*-toluenesulfonic acid catalyst to pack a ceramic membrane tube for the transesterification of a recirculating

Open Access Article. Published on 24 June 2014. Downloaded on 1/3/2025 11:41:55 PM.
This article is licensed under a Creative Commons Attribution 3.0 Unported Licence.

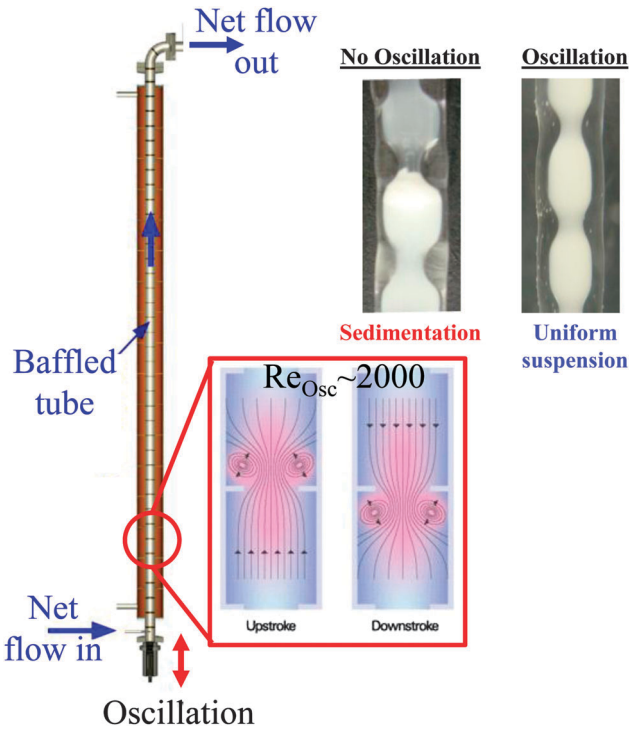

Fig. 18 Schematic of reactor flow and mixing characteristics within an OBR, and associated optical images of a $PrSO_3H$-SBA-15 solid acid powder without oscillation (undergoing sedimentation) or with a 4.5 Hz oscillation (entrained within baffles). Adapted from ref. 42 with permission from The Royal Society of Chemistry.

soybean oil and methanol feed (Fig. 19a). A higher biodiesel yield was obtained with the membrane reactor than with a homogeneous *p*-toluenesulfonic acid catalyst under comparable conditions in batch mode (84 *versus* 66%). Catalyst re-used evidenced only a minor loss of activity (92% of original after the third cycle).[254] Biodiesel yield was a strong function of circulation velocity; low velocities improved permeation efficiency, while high velocities enhanced reactant mixing intensity. Although membrane reactors offer efficient transesterification and separation, they require high catalyst volumes, for example a 202 cm^3 continuous reactor employed 157 g of a microporous TiO_2/Al_2O_3 membrane packed with potassium hydroxide supported on palm shell activated carbon to produce high quality methyl esters from palm oil (Fig. 19b).[252]

Enzymatic catalysed biodiesel production has been reported in both continuous[257,258] and batch modes.[259] Nature has developed a range of lipase biocatalysts for the selective synthesis of FAME at low reaction temperature, which are tolerate to high FFA levels.[260,261] Immobilisation on solid supports enables such biocatalysts to be used in continuous mode with low methanol : oil ratios.[262] However, there are numerous shortcomings of biocatalysts including high enzyme costs, long residence times, and low biodiesel yields. Some enzymes can also be deactivated by short chain alcohols and the glycerol by-product;[263] this problem can be overcome through the use of organic solvents to extract the alcohols and glycerol, but this adds further complexity and cost, and weakens the green credentials of biodiesel production. Enzymes must also operate in the presence of water in order to avoid denaturation, however this additional water must be subsequently removed from the resulting fuel to meet biodiesel standards (<0.05 vol% H_2O), these drying steps introducing further costs. An alternative approach is the use of near-critical[264] or supercritical CO_2[255,256] as a reaction medium to minimise enzyme inhibition by methanol, enhance oil solubility and diffusion, and assist catalyst/biodiesel separation *via* simple depressurisation. The associated strengths and weaknesses of supercritical biodiesel production are reviewed elsewhere.[265]

Ultrasound[266,267] and microwaves[268,269] have been explored as a means of eliminating heat and mass transfer limitations, and shortening residence times to achieve high biodiesel conversions. Ultrasound was used by Gude *et al.* in place of thermal heating for the transesterification of waste cooking oil,[266] allowing efficient heating to a temperature of 60–65 °C and lowering reaction times to 1–2 min. Chand *et al.* observed similar improvements in heat transfer and reaction time applying ultrasonication to soybean oil transesterification.[270] However, both groups employed a homogeneous NaOH catalyst, hindering product purification. Ultrasound was used with a heterogeneous catalyst for continuous biodiesel production from palm oil by Salamatinia *et al.*[271] BaO and SrO catalysts were tested, and ultrasound again found to reduce the reaction times and catalyst loadings needed to achieve >95% FAME yields.

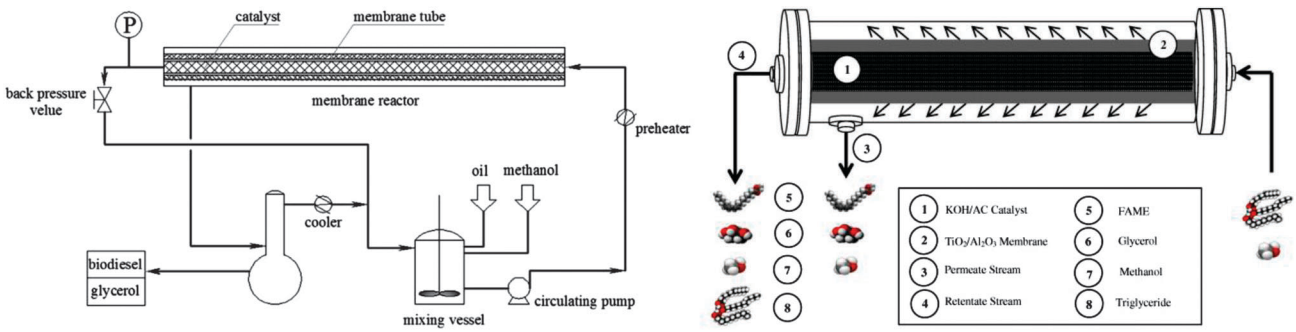

Fig. 19 Schematic of recirculating packed membrane reactors for continuous biodiesel production *via* (a) solid acid and (b) base catalysts. Reprinted from ref. 252 and 254. Copyright (2011 and 2014), with permission from Elsevier.

Open Access Article. Published on 24 June 2014. Downloaded on 1/3/2025 11:41:55 PM.
This article is licensed under a Creative Commons Attribution 3.0 Unported Licence.

Cost analysis of an ultrasonic process suggests it would be at least three times more expensive to run than a conventionally heated continuous biodiesel reactor.[270] The origin of ultrasonic enhancements in respect of reaction mixing *via e.g.* cavitation or microstreaming, remains a matter of debate.[272] Microwaves have been coupled with continuous flow reactors for the transesterification of waste cooking oil, accelerating biodiesel production compared to conventional thermal heating, and hence higher throughput.[269] The majority of microwave studies to date have focused on homogeneously catalysed processes, although some innovative combinations of waste derived (eggshell) solid catalysts and microwaves are emerging.[273] Such microwave systems also require less solvent and catalyst. However, microwave penetration depth is a limiting factor[268] which may restrict scale-up from laboratory reactor designs, and uncontrolled and irregular heat distribution can result in 'hot spots' and 'cold spots'.[267,268]

7. Future directions

If sourced and produced in a sustainable fashion, biodiesel has the potential to play an important role in meeting renewable fuel targets. However, developments in materials design and construction are critical to achieve significant improvements in heterogeneously catalysed biodiesel production. Designer solid acid and base catalysts with tailored surface properties and pore networks offer process improvements over existing, commercial homogeneous catalysed production employing liquid bases, facilitating simple catalyst separation and fuel purification, coupled with continuous biodiesel synthesis. Tuning the surface hydrophobicity of heterogeneous catalysts can strongly influence oil transesterification and FFA esterification through the expulsion of water away from active catalytic centres, thus limiting undesired reverse hydrolysis processes, notably in high water content waste oils. Solid materials capable of simultaneous FFA esterification and TAG transesterification under mild conditions present a major challenge for catalytic scientists, although (insoluble) high area superacids represent a step in this direction. We predict that in the future, hierarchical solid acids may be employed to first hydrolyse non-edible oil feedstocks, and subsequently esterify the resulting FFAs to FAME. Synthesis of nanostructured (*e.g.* nanocrystalline) catalysts and the application of surface-initiated, controlled polymerisation to functionalise oxide surfaces with polymeric organic species to create hybrid organic–inorganic architectures with high active site loadings, will prove valuable in the quest for enhanced catalyst performance.

Despite concerns over long term biodiesel use in high performance engines, the implementation of FAME containing longer chain ($>C_{18}$) esters in heavy-duty diesel engines should prove less problematic to on short timecales. However, the widespread uptake and development of next-generation biodiesel fuels requires progressive government policies and incentive schemes to place biodiesel on a comparative footing with (heavily subsidised) fossil-fuels. Blending of biodiesel with pyrolysis oil derived from lignocellulosic waste is an attractive route to power low-medium scale Combined Heat and Power (CHP) engines. Increasing use of waste or low grade oil sources remains a challenge for existing heterogeneous catalysts, since the high concentration of impurities (acid, moisture, heavy metals) induce rapid on-stream deactivation, and necessitate improved upstream oil purification, or more robust catalyst formulations tolerant to such components. Feedstock selection is dominated by regional availability, however the drive to use non-edible oil sources in areas where they cannot be readily sourced will require close attention to the entire supply chain and emissions/costs associated with new transportation networks, and may favour genetic modification of plant and algal strains to adapt to non-native climates.

The viscosity and attendant poor miscibility of many oil feedstocks with light alcohols continues to hamper the use of new heterogeneous catalysts for continuous biodiesel production, from both a materials and engineering perspective. Future process optimisation and growth in biodiesel supply and demand needs a concerted effort between catalyst chemists, chemical engineers and experts in molecular simulation in order to take advantage of innovative reactor designs and develop catalysts and reactors in tandem. Alternative reactor technologies and process intensification *via e.g.* reactive distillation and oscillatory flow reactors will facilitate distributed biodiesel production. It is essential that technical advances in both materials chemistry and reactor engineering are pursued if biodiesel is to remain a key player in the renewable energy sector during the 21st century.

Acknowledgements

A.F.L. thanks the EPSRC for the award of a Leadership Fellowship (EP/G007594/4). K.W. thanks the Royal Society for the award of an Industry Fellowship.

References

1 S. Kretzmann, http://priceofoil.org/2013/11/26/new-analysis-shows-growing-fossil-reserves-shrinking-carbon-budget/.
2 C. C. Authority, Reducing Australia's Greenhouse Gas Emissions – Targets and Progress Review Draft Report, Commonwealth of Australia, 2013.
3 C. C. Secretariat, The critical decade 2013 Climate change science, risks and responses, Commonwealth of Australia, 2013.
4 I. E. Agency, *Prospect of limiting the global increase in temperature to 2 °C is getting bleaker*, http://www.iea.org/newsroomandevents/news/2011/may/name,19839,en.html.
5 I. E. Agency, Redrawing the Energy Climate Map, 2013.
6 U. S. E. I. Administration, *International Energy Outlook 2013*, 2013.
7 PwC, World in 2050. The BRICs and beyond: prospects, challenges and opportunities, 2013.
8 N. Armaroli and V. Balzani, *Angew. Chem., Int. Ed.*, 2007, **46**, 52–66.

Open Access Article. Published on 24 June 2014. Downloaded on 1/3/2025 11:41:55 PM.
This article is licensed under a Creative Commons Attribution 3.0 Unported Licence.

9 P. Azadi, O. R. Inderwildi, R. Farnood and D. A. King, *Renewable Sustainable Energy Rev.*, 2013, **21**, 506–523.
10 J. M. Thomas, *Proceedings of the Royal Society A: Mathematical, Physical and Engineering Science*, 2012, **468**, 1884–1903.
11 G. A. Somorjai, H. Frei and J. Y. Park, *J. Am. Chem. Soc.*, 2009, **131**, 16589–16605.
12 A. Demirbas, *Energy Policy*, 2007, **35**, 4661–4670.
13 T. P. Vispute, H. Zhang, A. Sanna, R. Xiao and G. W. Huber, *Science*, 2010, **330**, 1222–1227.
14 P. M. Mortensen, J. D. Grunwaldt, P. A. Jensen, K. G. Knudsen and A. D. Jensen, *Appl. Catal., A*, 2011, **407**, 1–19.
15 R. Luque, L. Herrero-Davila, J. M. Campelo, J. H. Clark, J. M. Hidalgo, D. Luna, J. M. Marinas and A. A. Romero, *Energy Environ. Sci.*, 2008, **1**, 542–564.
16 C. S. K. Lin, L. A. Pfaltzgraff, L. Herrero-Davila, E. B. Mubofu, S. Abderrahim, J. H. Clark, A. A. Koutinas, N. Kopsahelis, K. Stamatelatou, F. Dickson, S. Thankappan, Z. Mohamed, R. Brocklesby and R. Luque, *Energy Environ. Sci.*, 2013, **6**, 426–464.
17 D. W. McLaughlin, *Conserv. Biol.*, 2011, **25**, 1117–1120.
18 F. Danielsen, H. Beukema, N. D. Burgess, F. Parish, C. A. Brühl, P. F. Donald, D. Murdiyarso, B. E. N. Phalan, L. Reijnders, M. Struebig and E. B. Fitzherbert, *Conserv. Biol.*, 2009, **23**, 348–358.
19 W. M. J. Achten, L. Verchot, Y. J. Franken, E. Mathijs, V. P. Singh, R. Aerts and B. Muys, *Biomass Bioenergy*, 2008, **32**, 1063–1084.
20 T. M. Mata, A. A. Martins and N. S. Caetano, *Renewable Sustainable Energy Rev.*, 2010, **14**, 217–232.
21 BP, *BP Energy Outlook 2030*, 2011.
22 G. Knothe, *Top. Catal.*, 2010, **53**, 714–720.
23 M. J. Climent, A. Corma, S. Iborra and A. Velty, *J. Catal.*, 2004, **221**, 474–482.
24 U. Constantino, F. Marmottini, M. Nocchetti and R. Vivani, *Eur. J. Inorg. Chem.*, 1998, 1439–1446.
25 K. Narasimharao, A. Lee and K. Wilson, *J. Biobased Mater. Bioenergy*, 2007, **1**, 19–30.
26 M. R. Othman, Z. Helwani, Martunus and W. J. N. Fernando, *Appl. Organomet. Chem.*, 2009, **23**, 335–346.
27 Y. Liu, E. Lotero, J. G. Goodwin and X. Mo, *Appl. Catal., A*, 2007, **33**, 138–148.
28 J. Geuens, J. M. Kremsner, B. A. Nebel, S. Schober, R. A. Dommisse, M. Mittelbach, S. Tavernier, C. O. Kappe and B. U. W. Maes, *Energy Fuels*, 2007, **22**, 643–645.
29 J. Hu, Z. Du, Z. Tang and E. Min, *Ind. Eng. Chem. Res.*, 2004, **43**, 7928–7931.
30 G. Knothe, *Fuel Process. Technol.*, 2005, **86**, 1059–1070.
31 F. Ma and M. A. Hanna, *Bioresour. Technol.*, 1999, **70**, 1–15.
32 E. Lotero, Y. Liu, D. E. Lopez, K. Suwannakarn, D. A. Bruce and J. G. Goodwin, *Ind. Eng. Chem. Res.*, 2005, **44**, 5353–5363.
33 R. Luque, J. C. Lovett, B. Datta, J. Clancy, J. M. Campelo and A. A. Romero, *Energy Environ. Sci.*, 2010, **3**, 1706–1721.
34 J.-P. Dacquin, A. F. Lee and K. Wilson, *Thermochemical Conversion of Biomass to Liquid Fuels and Chemicals*, The Royal Society of Chemistry, 2010, pp. 416–434.
35 K. Wilson and A. F. Lee, *Catal. Sci. Technol.*, 2012, **2**, 884.
36 L. J. Konwar, J. Boro and D. Deka, *Renewable Sustainable Energy Rev.*, 2014, **29**, 546–564.
37 A. Islam, Y. H. Taufiq-Yap, C.-M. Chu, E.-S. Chan and P. Ravindra, *Process Saf. Environ. Prot.*, 2013, **91**, 131–144.
38 K. Ramachandran, T. Suganya, N. Nagendra Gandhi and S. Renganathan, *Renewable Sustainable Energy Rev.*, 2013, **22**, 410–418.
39 Y. M. Sani, W. M. A. W. Daud and A. R. Abdul Aziz, *Appl. Catal., A*, 2014, **470**, 140–161.
40 I. M. Atadashi, M. K. Aroua, A. R. Abdul Aziz and N. M. N. Sulaiman, *J. Ind. Eng. Chem.*, 2013, **19**, 14–26.
41 Y. M. Sani, W. M. A. W. Daud and A. R. Abdul Aziz, *J. Environ. Chem. Eng.*, 2013, **1**, 113–121.
42 V. C. Eze, A. N. Phan, C. Pirez, A. P. Harvey, A. F. Lee and K. Wilson, *Catal. Sci. Technol.*, 2013, **3**, 2373–2379.
43 S. P. Singh and D. Singh, *Renewable Sustainable Energy Rev.*, 2010, **14**, 200–216.
44 P. Schenk, S. Thomas-Hall, E. Stephens, U. Marx, J. Mussgnug, C. Posten, O. Kruse and B. Hankamer, *BioEnergy Res.*, 2008, **1**, 20–43.
45 R. E. H. Sims, W. Mabee, J. N. Saddler and M. Taylor, *Bioresour. Technol.*, 2010, **101**, 1570–1580.
46 J. Kansedo, K. T. Lee and S. Bhatia, *Biomass Bioenergy*, 2009, **33**, 271–276.
47 J. M. Encinar, J. F. Gonzalez, A. Pardal and G. Martinez, *Fuel Process. Technol.*, 2010, **91**, 1530–1536.
48 J. Calero, D. Luna, E. D. Sancho, C. Luna, F. M. Bautista, A. A. Romero, A. Posadillo and C. Verdugo, *Fuel*, 2014, **122**, 94–102.
49 V. Scholz and J. N. da Silva, *Biomass Bioenergy*, 2008, **32**, 95–100.
50 E. Akbar, Z. Yaakob, S. K. Kamarudin, M. Ismail and J. Salimon, *Eur. J. Sci. Res.*, 2009, **29**, 396–403.
51 A. Karmakar, S. Karmakar and S. Mukherjee, *Renewable Sustainable Energy Rev.*, 2012, **16**, 1050–1060.
52 Y. Chisti, *Biotechnol. Adv.*, 2007, **25**, 294–306.
53 H. N. Bhatti, M. A. Hanif, M. Qasim and R. Ataur, *Fuel*, 2008, **87**, 2961–2966.
54 D. M. Kargbo, *Energy Fuels*, 2010, **24**, 2791–2794.
55 D. Frieden, N. Pena, D. N. Bird, H. Schwaiger and L. Canella, *Center for International Forestry Research (CIFOR)*, Bogor, Indonesia, 2011, p. 61.
56 L. Lardon, A. Hélias, B. Sialve, J.-P. Steyer and O. Bernard, *Environ. Sci. Technol.*, 2009, **43**, 6475–6481.
57 ASTM Standard D6751, *Standard Specification for Biodiesel Fuel Blend Stock (B100) for Middle Distillate Fuels*, ASTM International, West Conshohocken, PA, 2012, DOI: 0.1520/D6751-12, www.astm.org.
58 ASTM Standard D6751, *Standard Specification for Biodiesel Fuel Blend Stock (B100) for Middle Distillate Fuels*, ASTM International, West Conshohocken, PA, 2012, DOI: 0.1520/D6751-12, www.astm.org.
59 D. Y. C. Leung, X. Wu and M. K. H. Leung, *Appl. Energy*, 2010, **87**, 1083–1095.
60 Y. C. Sharma and B. Singh, *Renewable Sustainable Energy Rev.*, 2009, **13**, 1646–1651.

Open Access Article. Published on 24 June 2014. Downloaded on 1/3/2025 11:41:55 PM.
This article is licensed under a Creative Commons Attribution 3.0 Unported Licence.

61 A. Demirbas, *Energy Convers. Manage.*, 2009, **50**, 14–34.
62 A. Elbehri, A. Segerstedt and P. Liu, *Biodiesel and sustainability challenge: A global assessment of sustainability issues, trends and policies for biofuels and related feedstocks*, Food and Agriculture Organization of the United Nations, 2013.
63 R. Sarin, M. Sharma, S. Sinharay and R. K. Malhotra, *Fuel*, 2007, **86**, 1365–1371.
64 M. K. Lam, K. T. Lee and A. R. Mohamed, *Biotechnol. Adv.*, 2010, **28**, 500–518.
65 J. C. Escobar, E. S. Lora, O. J. Venturini, E. E. Yáñez, E. F. Castillo and O. Almazan, *Renewable Sustainable Energy Rev.*, 2009, **13**, 1275–1287.
66 N. H. Tran, J. R. Bartlett, G. S. K. Kannangara, A. S. Milev, H. Volk and M. A. Wilson, *Fuel*, 2010, **89**, 265–274.
67 G. Knothe, *Green Chem.*, 2011, **13**, 3048–3065.
68 A. Karmakar, S. Karmakar and S. Mukherjee, *Bioresour. Technol.*, 2010, **101**, 7201–7210.
69 *The Biodiesel Handbook*, AOCS Publishing, 2005.
70 T. P. Durrett, C. Benning and J. Ohlrogge, *Plant J.*, 2008, **54**, 593–607.
71 E. N. Frankel, *Lipid Oxidation*, The Oily Press, Bridgewater, England, 2nd edn, 2005.
72 C. A. W. Allen, K. C. Watts, R. G. Ackman and M. J. Pegg, *Fuel*, 1999, **78**, 1319–1326.
73 G. Knothe and K. R. Steidley, *Energy Fuels*, 2005, **19**, 1192–1200.
74 G. Knothe, S. C. Cermak and R. L. Evangelista, *Energy Fuels*, 2009, **23**, 1743–1747.
75 R. Radakovits, R. E. Jinkerson, A. Darzins and M. C. Posewitz, *Eukaryotic Cell*, 2010, **9**, 486–501.
76 Y. Ono and T. Baba, *Catal. Today*, 1997, **38**, 321–337.
77 H. Hattori, *Chem. Rev.*, 1995, **95**, 537–558.
78 M. C. G. Albuquerque, D. C. S. Azevedo, C. L. Cavalcante Jr, J. Santamaría-González, J. M. Mérida-Robles, R. Moreno-Tost, E. Rodríguez-Castellón, A. Jiménez-López and P. Maireles-Torres, *J. Mol. Catal. A: Chem.*, 2009, **300**, 19–24.
79 G. R. Peterson and W. P. Scarrah, *J. Am. Oil Chem. Soc.*, 1984, **61**, 1593–1597.
80 M. Verziu, S. M. Coman, R. Richards and V. I. Parvulescu, *Catal. Today*, 2011, **167**, 64–70.
81 M. López Granados, D. Martin Alonso, A. C. Alba-Rubio, R. Mariscal, M. Ojeda and P. Brettes, *Energy Fuels*, 2009, **23**, 2259–2263.
82 M. Di Serio, R. Tesser, L. Casale, A. Dapos;Angelo, M. Trifuoggi and E. Santacesaria, *Top. Catal.*, 2010, **53**, 811–819.
83 M. Su, R. Yang and M. Li, *Fuel*, 2013, **103**, 398–407.
84 C. S. MacLeod, A. P. Harvey, A. F. Lee and K. Wilson, *Chem. Eng. J.*, 2008, **135**, 63–70.
85 J. Montero, K. Wilson and A. Lee, *Top. Catal.*, 2010, **53**, 737–745.
86 R. S. Watkins, A. F. Lee and K. Wilson, *Green Chem.*, 2004, **6**, 335–340.
87 D. M. Alonso, R. Mariscal, M. L. Granados and P. Maireles-Torres, *Catal. Today*, 2009, **143**, 167–171.
88 M. Verziu, B. Cojocaru, J. Hu, R. Richards, C. Ciuculescu, P. Filip and V. I. Parvulescu, *Green Chem.*, 2008, **10**, 373–381.
89 K. Zhu, J. Hu, C. Kübel and R. Richards, *Angew. Chem., Int. Ed.*, 2006, **45**, 7277–7281.
90 J. M. Montero, P. Gai, K. Wilson and A. F. Lee, *Green Chem.*, 2009, **11**, 265–268.
91 J. M. Montero, D. R. Brown, P. L. Gai, A. F. Lee and K. Wilson, *Chem. Eng. J.*, 2010, **161**, 332–339.
92 J. J. Woodford, C. M. A. Parlett, J.-P. Dacquin, G. Cibin, A. Dent, J. Montero, K. Wilson and A. F. Lee, *J. Chem. Technol. Biotechnol.*, 2014, **89**, 73–80.
93 Y. L. Meng, B. Y. Wang, S. F. Li, S. J. Tian and M. H. Zhang, *Bioresour. Technol.*, 2013, **128**, 305–309.
94 W. Xie and L. Zhao, *Energy Convers. Manage.*, 2014, **79**, 34–42.
95 W. Xie and L. Zhao, *Energy Convers. Manage.*, 2013, **76**, 55–62.
96 E. Rashtizadeh, F. Farzaneh and Z. Talebpour, *Bioresour. Technol.*, 2013, **154C**, 32–37.
97 J.-X. Wang, K.-T. Chen, J.-S. Wu, P.-H. Wang, S.-T. Huang and C.-C. Chen, *Fuel Process. Technol.*, 2012, **104**, 167–173.
98 Y.-D. Long, F. Guo, Z. Fang, X.-F. Tian, L.-Q. Jiang and F. Zhang, *Bioresour. Technol.*, 2011, **102**, 6884–6886.
99 Y.-D. Long, Z. Fang, T.-C. Su and Q. Yang, *Appl. Energy*, 2014, **113**, 1819–1825.
100 T. M. Barnard, N. E. Leadbeater, M. B. Boucher, L. M. Stencel and B. A. Wilhite, *Energy Fuels*, 2007, **21**, 1777–1781.
101 X.-f. Li, Y. Zuo, Y. Zhang, Y. Fu and Q.-x. Guo, *Fuel*, 2013, **113**, 435–442.
102 X. Liang, S. Gao, H. Wu and J. Yang, *Fuel Process. Technol.*, 2009, **90**, 701–704.
103 H. Wu, J. Zhang, Y. Liu, J. Zheng and Q. Wei, *Fuel Process. Technol.*, 2014, **119**, 114–120.
104 Y. Li, W. Zhang, L. Zhang, Q. Yang, Z. Wei, Z. Feng and C. Li, *J. Phys. Chem. B*, 2004, **108**, 9739–9744.
105 W. Xie and M. Fan, *Chem. Eng. J.*, 2014, **239**, 60–67.
106 K.-T. Chen, J.-X. Wang, Y.-M. Dai, P.-H. Wang, C.-Y. Liou, C.-W. Nien, J.-S. Wu and C.-C. Chen, *J. Taiwan Inst. Chem. Eng.*, 2013, **44**, 622–629.
107 F. A. Dawodu, O. Ayodele, J. Xin, S. Zhang and D. Yan, *Appl. Energy*, 2014, **114**, 819–826.
108 X. Fu, D. Li, J. Chen, Y. Zhang, W. Huang, Y. Zhu, J. Yang and C. Zhang, *Bioresour. Technol.*, 2013, **146**, 767–770.
109 B. L. A. Prabhavathi Devi, T. Vijai Kumar Reddy, K. Vijaya Lakshmi and R. B. N. Prasad, *Bioresour. Technol.*, 2013, **153**, 370–373.
110 Y. Shen, P. Zhao and Q. Shao, *Microporous Mesoporous Mater.*, 2014, **188**, 46–76.
111 K. Gombotz, R. Parette, G. Austic, D. Kannan and J. V. Matson, *Fuel*, 2012, **92**, 9–15.
112 A. Molaei Dehkordi and M. Ghasemi, *Fuel Process. Technol.*, 2012, **97**, 45–51.
113 N. Santiago-Torres, I. C. Romero-Ibarra and H. Pfeiffer, *Fuel Process. Technol.*, 2014, **120**, 34–39.
114 G. G. Santillán-Reyes and H. Pfeiffer, *Int. J. Greenhouse Gas Control*, 2011, **5**, 1624–1629.
115 P. Hernández-Hipólito, M. García-Castillejos, E. Martínez-Klimova, N. Juárez-Flores, A. Gómez-Cortés and T. E. Klimova, *Catal. Today*, 2014, **220–222**, 4–11.

Open Access Article. Published on 24 June 2014. Downloaded on 1/3/2025 11:41:55 PM.
This article is licensed under a Creative Commons Attribution 3.0 Unported Licence.

116 D. G. Cantrell, L. J. Gillie, A. F. Lee and K. Wilson, *Appl. Catal., A*, 2005, **287**, 183–190.
117 M. Di Serio, M. Ledda, M. Cozzolino, G. Minutillo, R. Tesser and E. Santacesaria, *Ind. Eng. Chem. Res.*, 2006, **45**, 3009–3014.
118 F. Cavani, F. Trifirò and A. Vaccari, *Catal. Today*, 1991, **11**, 173–301.
119 N. Barakos, S. Pasias and N. Papayannakos, *Bioresour. Technol.*, 2008, **99**, 5037–5042.
120 J. M. Fraile, N. García, J. A. Mayoral, E. Pires and L. Roldán, *Appl. Catal., A*, 2009, **364**, 87–94.
121 H. E. Cross and D. R. Brown, *Catal. Commun.*, 2010, **12**, 243–245.
122 T. Hibino and M. Kobayashi, *J. Mater. Chem.*, 2005, **15**, 653–656.
123 J. M. Hidalgo, C. Jiménez-Sanchidrián and J. R. Ruiz, *Appl. Catal., A*, 2014, **470**, 311–317.
124 J. J. Creasey, A. Chieregato, J. C. Manayil, C. M. A. Parlett, K. Wilson and A. F. Lee, *Catal. Sci. Technol.*, 2014, **4**, 861–870.
125 E. Géraud, V. Prévot, J. Ghanbaja and F. Leroux, *Chem. Mater.*, 2005, **18**, 238–240.
126 E. Géraud, S. Rafqah, M. Sarakha, C. Forano, V. Prevot and F. Leroux, *Chem. Mater.*, 2007, **20**, 1116–1125.
127 J. J. Woodford, J.-P. Dacquin, K. Wilson and A. F. Lee, *Energy Environ. Sci.*, 2012, **5**, 6145–6150.
128 M. N. V. Ravi Kumar, U. Bakowsky and C. M. Lehr, *Biomaterials*, 2004, **25**, 1771–1777.
129 D. Highley, A. Bloodworth and R. Bate, *Dolomite-Mineral planning factsheet*, British Geological Survey, 2006.
130 D. Sutton, B. Kelleher and J. R. H. Ross, *Fuel Process. Technol.*, 2001, **73**, 155–173.
131 K. Wilson, C. Hardacre, A. F. Lee, J. M. Montero and L. Shellard, *Green Chem.*, 2008, **10**, 654–659.
132 O. Ilgen, *Fuel Process. Technol.*, 2011, **92**, 452–455.
133 Z. A. Shajaratun Nur, Y. H. Taufiq-Yap, M. F. Rabiah Nizah, S. H. Teo, O. N. Syazwani and A. Islam, *Energy Convers. Manage.*, 2014, **78**, 738–744.
134 P. Zhang, Q. Han, M. Fan and P. Jiang, *Fuel*, 2014, **124**, 66–72.
135 E. Karimi, I. F. Teixeira, L. P. Ribeiro, A. Gomez, R. M. Lago, G. Penner, S. W. Kycia and M. Schlaf, *Catal. Today*, 2012, **190**, 73–88.
136 E. Karimi, A. Gomez, S. W. Kycia and M. Schlaf, *Energy Fuels*, 2010, **24**, 2747–2757.
137 K. Narasimharao, D. R. Brown, A. F. Lee, A. D. Newman, P. F. Siril, S. J. Tavener and K. Wilson, *J. Catal.*, 2007, **248**, 226–234.
138 K. Suwannakarn, E. Lotero, K. Ngaosuwan and J. G. Goodwin, *Ind. Eng. Chem. Res.*, 2009, **48**, 2810–2818.
139 M. Kouzu, A. Nakagaito and J.-s. Hidaka, *Appl. Catal., A*, 2011, **405**, 36–44.
140 D. Zhao, Q. Huo, J. Feng, B. F. Chmelka and G. D. Stucky, *J. Am. Chem. Soc.*, 1998, **120**, 6024–6036.
141 I. K. Mbaraka and B. H. Shanks, *J. Catal.*, 2005, **229**, 365–373.
142 J. A. Melero, L. F. Bautista, G. Morales, J. Iglesias and D. Briones, *Energy Fuels*, 2008, **23**, 539–547.
143 X.-R. Chen, Y.-H. Ju and C.-Y. Mou, *J. Phys. Chem. C*, 2007, **111**, 18731–18737.
144 I. K. Mbaraka, D. R. Radu, V. S. Y. Lin and B. H. Shanks, *J. Catal.*, 2003, **219**, 329–336.
145 D. Chen, Z. Li, Y. Wan, X. Tu, Y. Shi, Z. Chen, W. Shen, C. Yu, B. Tu and D. Zhao, *J. Mater. Chem.*, 2006, **16**, 1511–1519.
146 L. Cao, T. Man and M. Kruk, *Chem. Mater.*, 2009, **21**, 1144–1153.
147 A. Martin, G. Morales, F. Martinez, R. van Grieken, L. Cao and M. Kruk, *J. Mater. Chem.*, 2010, **20**, 8026–8035.
148 P. Zeigermann, S. Naumov, S. Mascotto, J. Kärger, B. M. Smarsly and R. Valiullin, *Langmuir*, 2012, **28**, 3621–3632.
149 A. Vinu, N. Gokulakrishnan, V. V. Balasubramanian, S. Alam, M. P. Kapoor, K. Ariga and T. Mori, *Chem. – Eur. J.*, 2008, **14**, 11529–11538.
150 C. Pirez, J.-M. Caderon, J.-P. Dacquin, A. F. Lee and K. Wilson, *ACS Catal.*, 2012, **2**, 1607–1614.
151 D. E. López, J. G. Goodwin Jr, D. A. Bruce and E. Lotero, *Appl. Catal., A*, 2005, **295**, 97–105.
152 W. W. Mar and E. Somsook, *J. Oleo Sci.*, 2013, **62**, 435–442.
153 S.-Y. Chen, T. Mochizuki, Y. Abe, M. Toba and Y. Yoshimura, *Appl. Catal., B*, 2014, **148–149**, 344–356.
154 J. A. Melero, J. Iglesias and G. Morales, *Green Chem.*, 2009, **11**, 1285–1308.
155 A. Carrero, G. Vicente, R. Rodríguez, M. Linares and G. L. del Peso, *Catal. Today*, 2011, **167**, 148–153.
156 J. Y. Ying, C. P. Mehnert and M. S. Wong, *Angew. Chem., Int. Ed.*, 1999, **38**, 56–77.
157 Y. Lu, *Angew. Chem., Int. Ed.*, 2006, **45**, 7664–7667.
158 S. Garg, K. Soni, G. M. Kumaran, R. Bal, K. Gora-Marek, J. K. Gupta, L. D. Sharma and G. M. Dhar, *Catal. Today*, 2009, **141**, 125–129.
159 S. Gheorghiu and M.-O. Coppens, *AIChE J.*, 2004, **50**, 812–820.
160 X. Zhang, F. Zhang and K.-Y. Chan, *Mater. Lett.*, 2004, **58**, 2872–2877.
161 J.-H. Sun, Z. Shan, T. Maschmeyer and M.-O. Coppens, *Langmuir*, 2003, **19**, 8395–8402.
162 J.-P. Dacquin, J. r. m. Dhainaut, D. Duprez, S. b. Royer, A. F. Lee and K. Wilson, *J. Am. Chem. Soc.*, 2009, **131**, 12896–12897.
163 J. Dhainaut, J.-P. Dacquin, A. F. Lee and K. Wilson, *Green Chem.*, 2010, **12**, 296–303.
164 R. Hong, T. Pan, J. Qian and H. Li, *Chem. Eng. J.*, 2006, **119**, 71–81.
165 M. L. Curri, R. Comparelli, P. D. Cozzoli, G. Mascolo and A. Agostiano, *Mater. Sci. Eng., C*, 2003, **23**, 285–289.
166 G. P. Fotou and S. E. Pratsinis, *Chem. Eng. Commun.*, 1996, **151**, 251–260.
167 S. Chakrabarti and B. Dutta, *J. Hazard. Mater.*, 2004, **112**, 269–278.
168 H. Yoshida, S. Takashi, C. Murata and T. Hattori, *J. Catal.*, 2003, **220**, 226–232.

 This journal is © The Royal Society of Chemistry 2014

Open Access Article. Published on 24 June 2014. Downloaded on 1/3/2025 11:41:55 PM.
This article is licensed under a Creative Commons Attribution 3.0 Unported Licence.

169 G. Corro, U. Pal and N. Tellez, *Appl. Catal., B*, 2013, **129**, 39–47.
170 G. Corro, F. Bañuelos, E. Vidal and S. Cebada, *Fuel*, 2014, **115**, 625–628.
171 C. Pirez, K. Wilson and A. F. Lee, *Green Chem.*, 2014, **16**, 197–202.
172 N. Mizuno and M. Misono, *Chem. Rev.*, 1998, **98**, 199–218.
173 I. V. Kozhevnikov, *Chem. Rev.*, 1998, **98**, 171–198.
174 A. D. Newman, D. R. Brown, P. Siril, A. F. Lee and K. Wilson, *Phys. Chem. Chem. Phys.*, 2006, **8**, 2893–2902.
175 A. D. Newman, A. F. Lee, K. Wilson and N. A. Young, *Catal. Lett.*, 2005, **102**, 45–50.
176 L. Pesaresi, D. R. Brown, A. F. Lee, J. M. Montero, H. Williams and K. Wilson, *Appl. Catal., A*, 2009, **360**, 50–58.
177 X. Duan, Y. Liu, Q. Zhao, X. Wang and S. Li, *RSC Adv.*, 2013, **3**, 13748–13755.
178 S. Singh and A. Patel, *J. Cleaner Prod.*, 2014, **72**, 46–56.
179 P. Xia, F. Liu, C. Wang, S. Zuo and C. Qi, *Catal. Commun.*, 2012, **26**, 140–143.
180 W. Liu, P. Yin, X. Liu, W. Chen, H. Chen, C. Liu, R. Qu and Q. Xu, *Energy Convers. Manage.*, 2013, **76**, 1009–1014.
181 R. Tesser, M. Di Serio, L. Casale, L. Sannino, M. Ledda and E. Santacesaria, *Chem. Eng. J.*, 2010, **161**, 212–222.
182 X. Liang, *Ind. Eng. Chem. Res.*, 2013, **52**, 6894–6900.
183 D. Zeng, S. Liu, W. Gong, G. Wang, J. Qiu and H. Chen, *Appl. Catal., A*, 2014, **469**, 284–289.
184 C. A. Deshmane, M. W. Wright, A. Lachgar, M. Rohlfing, Z. Liu, J. Le and B. E. Hanson, *Bioresour. Technol.*, 2013, **147**, 597–604.
185 D. D. Chabukswar, P. K. K. S. Heer and V. G. Gaikar, *Ind. Eng. Chem. Res.*, 2013, **52**, 7316–7326.
186 C. Poonjarernsilp, N. Sano and H. Tamon, *Appl. Catal., B*, 2014, **147**, 726–732.
187 F. H. Alhassan, R. Yunus, U. Rashid, K. Sirat, A. Islam, H. V. Lee and Y. H. Taufiq-Yap, *Appl. Catal., A*, 2013, **456**, 182–187.
188 W. Xie and T. Wang, *Fuel Process. Technol.*, 2013, **109**, 150–155.
189 R. Sheikh, M.-S. Choi, J.-S. Im and Y.-H. Park, *J. Ind. Eng. Chem.*, 2013, **19**, 1413–1419.
190 M. Farooq, A. Ramli and D. Subbarao, *J. Cleaner Prod.*, 2013, **59**, 131–140.
191 A. Talebian-Kiakalaieh, N. A. S. Amin and H. Mazaheri, *Appl. Energy*, 2013, **104**, 683–710.
192 S. Yan, C. DiMaggio, S. Mohan, M. Kim, S. Salley and K. Y. S. Ng, *Top. Catal.*, 2010, **53**, 721–736.
193 L. Peng, A. Philippaerts, X. Ke, J. Van Noyen, F. De Clippel, G. Van Tendeloo, P. A. Jacobs and B. F. Sels, *Catal. Today*, 2010, **150**, 140–146.
194 P. S. Sreeprasanth, R. Srivastava, D. Srinivas and P. Ratnasamy, *Appl. Catal., A*, 2006, **314**, 148–159.
195 Z. Helwani, M. R. Othman, N. Aziz, J. Kim and W. J. N. Fernando, *Appl. Catal., A*, 2009, **363**, 1–10.
196 S. Miao and B. H. Shanks, *Appl. Catal., A*, 2009, **359**, 113–120.
197 I. Jiménez-Morales, J. Santamaría-González, P. Maireles-Torres and A. Jiménez-López, *Appl. Catal., B*, 2011, **105**, 199–205.
198 Q. Shu, J. Gao, Z. Nawaz, Y. Liao, D. Wang and J. Wang, *Appl. Energy*, 2010, **87**, 2589–2596.
199 I. M. Atadashi, M. K. Aroua, A. R. Abdul Aziz and N. M. N. Sulaiman, *Renewable Sustainable Energy Rev.*, 2012, **16**, 3456–3470.
200 D. Kusdiana and S. Saka, *Bioresour. Technol.*, 2004, **91**, 289–295.
201 J. K. Satyarthi, D. Srinivas and P. Ratnasamy, *Energy Fuels*, 2010, **24**, 2154–2161.
202 Y. Liu, E. Lotero and J. G. Goodwin Jr, *J. Catal.*, 2006, **243**, 221–228.
203 D. M. Alonso, M. L. Granados, R. Mariscal and A. Douhal, *J. Catal.*, 2009, **262**, 18–26.
204 K. Wilson, A. Rénson and J. H. Clark, *Catal. Lett.*, 1999, **61**, 51–55.
205 B. Rác, P. Hegyes, P. Forgo and Á. Molnár, *Appl. Catal., A*, 2006, **299**, 193–201.
206 Q. Yang, J. Liu, J. Yang, M. P. Kapoor, S. Inagaki and C. Li, *J. Catal.*, 2004, **228**, 265–272.
207 Q. Yang, M. P. Kapoor, N. Shirokura, M. Ohashi, S. Inagaki, J. N. Kondo and K. Domen, *J. Mater. Chem.*, 2005, **15**, 666–673.
208 G. Morales, G. Athens, B. F. Chmelka, R. van Grieken and J. A. Melero, *J. Catal.*, 2008, **254**, 205–217.
209 R. Sánchez-Vázquez, C. Pirez, J. Iglesias, K. Wilson, A. F. Lee and J. A. Melero, *ChemCatChem*, 2013, **5**, 994–1001.
210 D. Margolese, J. A. Melero, S. C. Christiansen, B. F. Chmelka and G. D. Stucky, *Chem. Mater.*, 2000, **12**, 2448–2459.
211 I. Díaz, C. Márquez-Alvarez, F. Mohino, J. N. Pérez-Pariente and E. Sastre, *J. Catal.*, 2000, **193**, 283–294.
212 J.-P. Dacquin, H. E. Cross, D. R. Brown, T. Duren, J. J. Williams, A. F. Lee and K. Wilson, *Green Chem.*, 2010, **12**, 1383–1391.
213 C. Schumacher, J. Gonzalez, P. A. Wright and N. A. Seaton, *J. Phys. Chem. B*, 2005, **110**, 319–333.
214 D. Zuo, J. Lane, D. Culy, M. Schultz, A. Pullar and M. Waxman, *Appl. Catal., B*, 2013, **129**, 342–350.
215 L. Sherry and J. A. Sullivan, *Catal. Today*, 2011, **175**, 471–476.
216 J. A. Melero, R. van Grieken and G. Morales, *Chem. Rev.*, 2006, **106**, 3790–3812.
217 A. P. S. Chouhan and A. K. Sarma, *Renewable Sustainable Energy Rev.*, 2011, **15**, 4378–4399.
218 A. Macario, G. Giordano, B. Onida, D. Cocina, A. Tagarelli and A. M. Giuffrè, *Appl. Catal., A*, 2010, **378**, 160–168.
219 D. Srinivas and J. Satyarthi, *Catal. Surv. Asia*, 2011, **15**, 145–160.
220 F. Yan, Z. Yuan, P. Lu, W. Luo, L. Yang and L. Deng, *Renewable Energy*, 2011, **36**, 2026–2031.
221 T. Nakato, M. Kimura, S.-I. Nakata and T. Okuhara, *Langmuir*, 1998, **14**, 319–325.
222 A. Drelinkiewicz, Z. Kalemba-Jaje, E. Lalik and R. Kosydar, *Fuel*, 2014, **116**, 760–771.

Open Access Article. Published on 24 June 2014. Downloaded on 1/3/2025 11:41:55 PM.
This article is licensed under a Creative Commons Attribution 3.0 Unported Licence.

223 G. Morales, R. van Grieken, A. Martín and F. Martínez, *Chem. Eng. J.*, 2010, **161**, 388–396.
224 I. Noshadi, R. Kumar, B. Kanjilal, R. Parnas, H. Liu, J. Li and F. Liu, *Catal. Lett.*, 2013, **143**, 792–797.
225 L. Geng, G. Yu, Y. Wang and Y. Zhu, *Appl. Catal., A*, 2012, **427–428**, 137–144.
226 R. Liu, X. Wang, X. Zhao and P. Feng, *Carbon*, 2008, **46**, 1664–1669.
227 B. Chang, J. Fu, Y. Tian and X. Dong, *J. Phys. Chem. C*, 2013, **117**, 6252–6258.
228 M. Kotwal, A. Kumar and S. Darbha, *J. Mol. Catal. A: Chem.*, 2013, **377**, 65–73.
229 L. Deng, T. Tan, F. Wang and X. Xu, *Eur. J. Lipid Sci. Technol.*, 2003, **105**, 727–734.
230 M. Iso, B. Chen, M. Eguchi, T. Kudo and S. Shrestha, *J. Mol. Catal. B: Enzym.*, 2001, **16**, 53–58.
231 C.-H. Liu, C.-C. Huang, Y.-W. Wang, D.-J. Lee and J.-S. Chang, *Appl. Energy*, 2012, **100**, 41–46.
232 N. Dizge, B. Keskinler and A. Tanriseven, *Biochem. Eng. J.*, 2009, **44**, 220–225.
233 L. Guerreiro, P. M. Pereira, I. M. Fonseca, R. M. Martin-Aranda, A. M. Ramos, J. M. L. Dias, R. Oliveira and J. Vital, *Catal. Today*, 2010, **156**, 191–197.
234 X. Liu, H. He, Y. Wang, S. Zhu and X. Piao, *Fuel*, 2008, **87**, 216–221.
235 S. Yan, H. Lu and B. Liang, *Energy Fuels*, 2007, **22**, 646–651.
236 Q. Yang, J. Liu, L. Zhang and C. Li, *J. Mater. Chem.*, 2009, **19**, 1945–1955.
237 B. Karimi, H. M. Mirzaei and A. Mobaraki, *Catal. Sci. Technol.*, 2012, **2**, 828–834.
238 M. Bender, *Bioresour. Technol.*, 1999, **70**, 81–87.
239 T. Sakai, A. Kawashima and T. Koshikawa, *Bioresour. Technol.*, 2009, **100**, 3268–3276.
240 E. F. Aransiola, T. V. Ojumu, O. O. Oyekola, T. F. Madzimbamuto and D. I. O. Ikhu-Omoregbe, *Biomass Bioenergy*, 2014, **61**, 276–297.
241 M. B. Tasić, O. S. Stamenković and V. B. Veljković, *Energy Convers. Manage.*, 2014, **84**, 405–413.
242 Y. Cheng, Y. Feng, Y. Ren, X. Liu, A. Gao, B. He, F. Yan and J. Li, *Bioresour. Technol.*, 2012, **113**, 65–72.
243 A. A. Kulkarni, K.-P. Zeyer, T. Jacobs and A. Kienle, *Ind. Eng. Chem. Res.*, 2007, **46**, 5271–5277.
244 Ó. de la Iglesia, R. Mallada, M. Menéndez and J. Coronas, *Chem. Eng. J.*, 2007, **131**, 35–39.
245 A. A. Kiss, A. C. Dimian and G. Rothenberg, *Energy Fuels*, 2007, **22**, 598–604.
246 C. Buchaly, P. Kreis and A. Górak, *Ind. Eng. Chem. Res.*, 2011, **51**, 891–899.
247 Z. Qiu, L. Zhao and L. Weatherley, *Chemical Engineering and Processing: Process Intensification*, 2010, **49**, 323–330.
248 G. L. Maddikeri, A. B. Pandit and P. R. Gogate, *Ind. Eng. Chem. Res.*, 2012, **51**, 14610–14628.
249 X. Ni, M. R. Mackley, A. P. Harvey, P. Stonestreet, M. H. I. Baird and N. V. Rama Rao, *Chem. Eng. Res. Des.*, 2003, **81**, 373–383.
250 A. N. Phan, A. P. Harvey and V. Eze, *Chem. Eng. Technol.*, 2012, **35**, 1214–1220.
251 R. G. Nelson and S. A. Hower, Sixth national bioenergy conference, 1994.
252 S. Baroutian, M. K. Aroua, A. A. Raman and N. M. Sulaiman, *Bioresour. Technol.*, 2011, **102**, 1095–1102.
253 H. Falahati and A. Y. Tremblay, *Fuel*, 2012, **91**, 126–133.
254 W. Xu, L. Gao, S. Wang and G. Xiao, *Bioresour. Technol.*, 2014, **159**, 286–291.
255 P. Cao, A. Y. Tremblay, M. A. Dubé and K. Morse, *Ind. Eng. Chem. Res.*, 2007, **46**, 52–58.
256 P. Cao, A. Y. Tremblay and M. A. Dubé, *Ind. Eng. Chem. Res.*, 2009, **48**, 2533–2541.
257 P. Lozano, J. M. Bernal and M. Vaultier, *Fuel*, 2011, **90**, 3461–3467.
258 X. Wang, X. Liu, C. Zhao, Y. Ding and P. Xu, *Bioresour. Technol.*, 2011, **102**, 6352–6355.
259 D. Lv, W. Du, G. Zhang and D. Liu, *Process Biochem.*, 2010, **45**, 446–450.
260 A. Bajaj, P. Lohan, P. N. Jha and R. Mehrotra, *J. Mol. Catal. B: Enzym.*, 2010, **62**, 9–14.
261 L. A. Nelson, T. A. Foglia and W. N. Marmer, *J. Am. Oil Chem. Soc.*, 1996, **73**, 1191–1195.
262 Y. Watanabe, Y. Shimada, A. Sugihara, H. Noda, H. Fukuda and Y. Tominaga, *J. Am. Oil Chem. Soc.*, 2000, **77**, 355–360.
263 K. Bélafi-Bakó, F. Kovács, L. Gubicza and J. Hancsók, *Biocatal. Biotransform.*, 2002, **20**, 437–439.
264 M. Lee, D. Lee, J. Cho, S. Kim and C. Park, *Appl. Biochem. Biotechnol.*, 2013, **171**, 1118–1127.
265 K. T. Tan and K. T. Lee, *Renewable Sustainable Energy Rev.*, 2011, **15**, 2452–2456.
266 V. G. Gude and G. E. Grant, *Appl. Energy*, 2013, **109**, 135–144.
267 V. L. Gole and P. R. Gogate, *Chemical Engineering and Processing: Process Intensification*, 2012, **53**, 1–9.
268 A. Mazubert, C. Taylor, J. Aubin and M. Poux, *Bioresour. Technol.*, 2014, **161**, 270–279.
269 W. A. Wali, A. I. Al-Shamma'a, K. H. Hassan and J. D. Cullen, *J. Process Control*, 2012, **22**, 1256–1272.
270 P. Chand, V. R. Chintareddy, J. G. Verkade and D. Grewell, *Energy Fuels*, 2010, **24**, 2010–2015.
271 B. Salamatinia, H. Mootabadi, S. Bhatia and A. Z. Abdullah, *Fuel Process. Technol.*, 2010, **91**, 441–448.
272 H. A. Choudhury, S. Chakma and V. S. Moholkar, *Ultrason. Sonochem.*, 2014, **21**, 169–181.
273 P. Khemthong, C. Luadthong, W. Nualpaeng, P. Changsuwan, P. Tongprem, N. Viriya-empikul and K. Faungnawakij, *Catal. Today*, 2012, **190**, 112–116.

 This journal is © The Royal Society of Chemistry 2014